Heliyon 10 (2024) e26717

Contents lists available at ScienceDirect

Heliyon

journal homepage: www.cell.com/heliyon

Research article

Modeling canopy water content in the assessment for rainfall induced surface and groundwater nitrate contamination: The Bilate cropland sub watershed

Bereket Geberselassie Assa [a,b,*], Anirudh Bhowmick [a], Bisrat Elias Cholo [a]

[a] Arba Minch University, Water Technology Institute, Faculty of Meteorology and Hydrology, Arba Minch, Ethiopia
[b] Wolaita Soddo University, Faculty of Engineering, Department of Civil Engineering, Soddo, Ethiopia

ARTICLE INFO

Keywords:
GWR modeling
Monthly rainfall
Nitrate contamination
Nitrate leaching
MODIS-EVI

ABSTRACT

Nitrate contamination in surface and groundwater remains a widespread problem in agricultural watersheds is primarily associated to high levels of percolation or leakage from fertilized soil, which allows easy infiltration from soil into groundwater. This study was aimed to predict canopy water content to determine the nitrate contamination index resulting from nitrogen fertilizer loss in surface and groundwater. The study used Geographically Weighted Regression (GWR) model using MODIS 006 MOD13Q1-EVI Earth observation data, crop information and rainfall data. Satellite data collection was synchronized with regional crop calendars and calibrated to plant biomass. The average plant biomass during observed plant growth stages was between 0.19 kg/m^2 at the minimum and 0.57 kg/m^2 at the maximum. These values are based on the growth stages of crops and provide a solid basis for monitoring and validating crop water productivity data. The simulation results were validated with a high correlation coefficient ($R^2 = 0.996$, $P < 0.0005$) for the observed rainfall in the growing zone compared to the predicted canopy water content. The nitrate contamination index assessment was conducted in 2004, 2008, 2009, 2010, 2011, 2013, 2014, 2015, 2018 and 2020. Canopy water content and root zone seasonal water content were measured in (%) per portion as indicators of the NO_3^--N-nitrate contamination index in these years (0.391, 0.316, 0.298, 0.389, 0.380, 0.339, 0.242, 0.342 and 0.356).

1. Introduction

Water and agricultural products are the most important resources for human survival on earth [1,2]. Furthermore, the need for global food and water security has been highlighted [1–5] by the fact that increasing demand for agricultural goods in tropical areas has also led to increased nitrogen fertilizer use in the farmland [3,4]. While N fertilizers can increase crop yields, excessive use in cropland coupled with seasonal fluctuations in rainfall can have harmful environmental effects, including contamination of surface and groundwater with nitrates.

Nitrate runoff and leaching, which can contaminate surface and groundwater [6] through seasonal N application losses on cropland, is also one of the major global challenges in cropland watersheds [6–8]. Ethiopia is one of the emerging countries where the loss of agricultural land is becoming a problem that poses water and environmental risks [9–12]. In addition to the resulting pollution of

* Corresponding author. Arba Minch University, Water Technology Institute, Faculty of Meteorology and Hydrology, Arba Minch, Ethiopia.
E-mail addresses: prawti-069-12@amu.edu.et (B.G. Assa), anirudh.bhowmick@amu.edu.et (A. Bhowmick), bisrat.elias@amu.edu.et (B.E. Cholo).

https://doi.org/10.1016/j.heliyon.2024.e26717
Received 27 September 2023; Received in revised form 24 January 2024; Accepted 19 February 2024
Available online 23 February 2024

water supplies, it is closely linked to and contributes significantly to food insecurity in many developing countries due to inequality in agricultural production. Due to this inequality, the unbalanced trend in nitrogen fertilization management on agricultural lands has increased [10–13] the risk of nitrate contamination of surfaces and groundwater.

Climatic changes in the Bilate watershed [14] have been recognized in previous studies as having a climatic impact on nitrogen fertilizer loss from agricultural land [14,15]; however, considering the entire watershed as an agricultural area, its research still revealed a knowledge gap excluding crop species and growing season. Nitrogen loss from cropland is not continuous, so it is important to consider specific growing seasons, crop classification and biomass index [14]. This hypothesis helps calibrate model parameters and improves the accuracy of model predictions based on estimated plant canopy water content.

For the seasonal nitrate contamination index of cropland, it is important to understand the complex interrelationship between parameters such as water and nutrient transport in crops [16–21]. The current study addresses the challenge of predicting nitrogen runoff and leaching, emphasizing the significant influence of crop parameters and seasonal water balance. Spatial clarification of the relationship [22] between nitrogen nutrient runoff/leaching capacity and crop vegetation index is crucial for reliable farmland runoff and leaching indices [23]. Furthermore, the study examined the integrated effects of seasonal rainfall patterns on crop response [24] for nitrogen fertilization on arable land with regard to nitrate runoff/leaching. Using geographically weighted regression (GWR) [25,26], the research aimed to model plant canopy water content to improve the accuracy of estimating crop water balance. The ultimate goal was to predict the likelihood of nitrate contamination occurring in croplands within the Bilate watershed, particularly during the rainy season [27–31]. This research contributes to improving our understanding of nutrient dynamics and water management in agricultural ecosystems by providing answers. How geographically weighted regression (GWR) [32] can be used to model plant canopy water content and improve the accuracy of plant water balance estimation, with a particular focus on predicting nitrate pollution resulting from nitrogen fertilization in croplands, particularly during the rainy season.

Calculating plant biomass indices provides a way to establish a connection between plant water and nutrient use efficiency [27,30]. This relationship is particularly important for assessing seasonal nitrogen loss from cropland and its impact on the watershed. The seasonal biomass index [30,33,34] of cropland below 0.25 kg/m^2 under nitrogen management can serve as an indicator of soil demineralization [29], especially in nutrient management for the entire rainfed cropping system [33]. According to a few studies, rainy season cropping in the study area is exposed to leached soil nutrients, indicating that trends indicate additional application of nitrogen-N fertilizer on croplands in the Ethiopian Rift Valley region [35]. Therefore, it is more important to focus on the peak or wet season when measuring nitrogen loss from agricultural land through runoff and leaching. Nitrogen nitrate leaching and runoff [31,36,

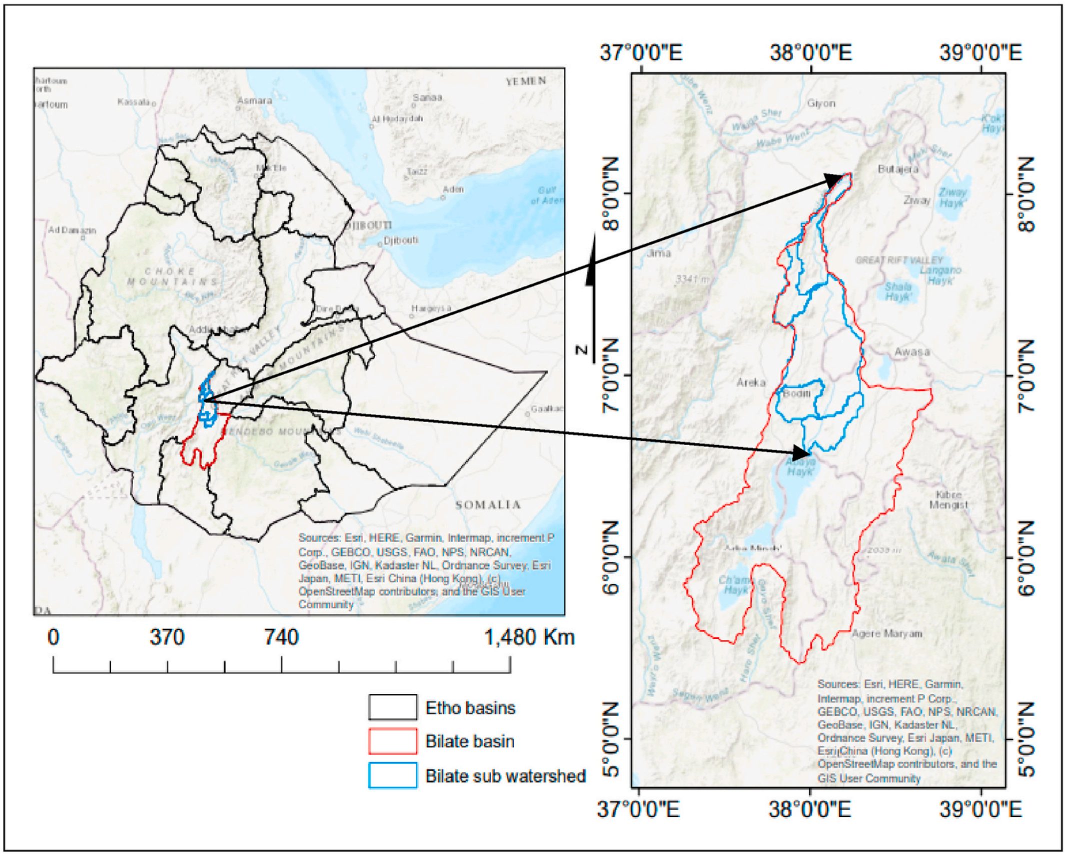

Fig. 1. Location map of the study area (Bilate sub watershed).

37]could be a source contributor to contaminating waterways, which largely depends on the growing season followed by heavy rainfall [34]. This supports the expectation of nitrogen-nitrate runoff and leaching loss from the highlands of the regional rainfed farming system in the Ethiopian Rift Valley [36]. Loss of N fertilizer on agricultural lands in agricultural watersheds exposed to (NO_3^--N) runoff or leaching was caused by a variety of factors, including climate, agricultural practices, trends in N fertilizer use and the type of agricultural terrain [22,31].

The study's current assumptions suggest that cropland is vulnerable to seasonal runoff and leaching of applied nitrogen fertilizer. This occurs when there is less water in the plant canopy than water in the growing zone during the under-rainfall period of a particular growing season [38,39]. Therefore, it is essential for the current study to evaluate the contribution of agricultural water balance [38–43] to surface and groundwater nitrate pollution [43]. Plant canopy water content must be lower than soil water content during rainfall in a given growing season to predict nitrate leaching runoff on agricultural land [44,45]. The Geographically Weighted Rogation (GWR) model was conceptually developed to determine seasonal canopy water content in cropping zone. Various data uncertainties that affect the simulation were taken into account, such as: Plant species, variations in zonal rainfall, soil type and slope. Consequently, the current study model aims to provide a more accurate and comprehensive assessment of plant canopy water content to predict the leaching flux of (NO_3^--N) from growing zones.

2. Materials and methods

2.1. Study area

The Bilate watershed (Fig. 1) is one of the sub-basins of the Rift Valley Lake basin and is located in the south-western part of the main catchments of the Ethiopian Rift Valley lakes [45]. The watershed originates from the Gurage Highlands and ends on the shores of Abaya Lake, comprising part of the SNNPR zones; Hadiya, KT, Gurage, Silte, Wolaita, Sidama and Alaba special woredas; and small parts of the south-central Oromiya regional states. The catchment area of Bilate River, which flows into Abaya Lake from the Gurage Highlands in the north of Abaya-Chamo Basin, accounts for about 38% of the Abaya Lake basin [46]. It is located between the coordinates 37,°47′6″ and 38,^{0}20′14″E and 6°33′18″ and 8°6′57″N, respectively. The watershed is situated within a region with a total area of 5504.29 km^2 and an altitude range of 1169–3276 m above sea level. The stream originates on the slope of the "Gurage" mountains and runs from the north. In addition to a stream that stretches for 197 km, the Guder and Weira tributaries of the Upper Bilate have exceptionally steep slopes, and their topography prohibits the use of storage basins. The stream at Bilate extends over 160 km, with the mean minimum and maximum discharge of the river being 0.413 m^3/s to 283.54 m^3/s. In the western highlands, the watershed is characterized by a humid climate. For season 1 or Belg, which ranges from March to April, the monthly rainfall, minimum temperature and maximum temperature data from 1998 to 2020 show a consistent pattern of monsoon rainfall. According to the agricultural growth curve, the ripening phase of crops is between May and July. There is a short dry season from November to February and a short rainy season from November to December. For years (1998–2020), monthly rainfall minimum and maximum data show an eight-month monomial rainfall pattern for the crop season beginning in March to April, the planting season, with a rainfall maximum between May and July [47–49] (time of maximum plant biomass index). And the dry season begins from November to February, with a shorter rainy season until early December.

3. Methodology

3.1. Data collection and analysis

The cropland biomass for a given cropland with a growing season for an annual time series was classified using [47,48,50–52] NASA Earth observation data with a spatial resolution of 250 m, specifically MODIS 006 MOD13Q1 [53]. For the current specific objective of conducting a simulation of crop water balance using the International Geosphere-Biosphere Program (IGBP), the validated

Table 1
Research data Specifications and use.

Data types	Specifications	Uses
Watershed Boundary	Shape file derived from 30 mR DEM GeoTiff, signed 16 bits, and 1 m/Digital Number using QSWAT	Developing watersheds to assess crop water balance, estimate contamination, and estimate effective rainfall observation stations for contamination estimation.
Land use Land cover for crop land	The International Geosphere Biosphere Programme (IGBP) has classified global vegetation for annual cropland in 500 mR (re-sampled to 250 mR) using MODIS-MCD12Q1 data.	Cropland area extraction to determine soil water content for specific crop types in the cropping zone.
Crop Biomass	MOD13Q1-MODIS 250 mR NASA earth data [52].	In order to calibrate total nitrogen use efficiency for Predicted canopy water content Nitrate contamination index [59]
Rainfall data Observation	Daily rainfall obstravtion from NMA (National Metriologe Agency) and active watershed gauge stations	Gauge stations are used for generating missing observations from CHIRPS daily observation [60,61]
Crop calendar	The crop calendar is used to determine the national crop pattern for the wet season [47] and regional crop calendar for cross validation [48].	Estimate rainfall based on calibrated active station from the NMA (National Meteorological Agency) and use to linke the Earth Engine Code Editor (google.com) to fill in any data gaps from selected observation stations.

classification of crop data [50] on land use and cover during the main growing season was adopted biomass level. Earth observation data from NASA Earth data, specifically MODIS 006 MOD13Q1 [49,54–56] with a spatial resolution of 250 m, were used to calculate zonal statistics for crop biomass index based on calibrated observations of study periods [48,54–58] (Table 1). This data was also used to classify cropland biomass in specific cropland areas. The growing season and the zonal statistics of the classified arable land areas with high and low arable biomass were taken into account to calibrate the model.

3.2. Crop data

The training data for classifying crop data (Fig. 2) [50] is used to integrate IGBP land use during the main cropping season and adopted for the current specific goal of conducting a simulation of crop water balance along with the International Geosphere-Biosphere Program (IGBP) to calibrate the model using the Enhanced Vegetation Index (EVI) of the MOD13Q1-EVI product [47,48]. This product has better sensitivity in regions with high biomass. The pixel value from the acquisitions of 16-day observations with low clouds, a low viewing angle, and the highest EVI value is used for the zonal statistics of the plant biomass index. The IGBP land use land cover class value [47] for observing cropland in time series was resampled to 250 m using the majority resampling technique algorithm to extract cropland within the watershed and converted into a shape file to provide information about the Type of crops to crop from Ethiopian Livelihood Zone data. Cropland was extracted from MODIS-MCD12Q1 of NASA Earth data [46,51] to create a land classification lookup table. Since cultivated area, cultivation dates and growing season are parameters and variables [56], it is important for modeling NO_3^--N occurrence through runoff leaching from the main agricultural watershed to downstream of the watershed. It can also lead to surface and groundwater pollution in downstream water resources. Therefore, in the current study, the cultivated area [ha] for the main rainy season was used as a crop parameter for plant biomass modeling. Since the nitrate pollution index for downstream water resources depends on N fertilizer input to croplands at agricultural watersheds [47,55], the IGBP cropland classification was used. Plant growth and biomass dynamics on the zonal mean of crops [56,62] depend on rainfall patterns and N application. The cropland for each plant species-based pixel of MODIS 250 m-EVI is used to analyse the plant biomass index [21,63].

3.3. Meteorological station

The National Meteorological Agency [64] of Ethiopia provided the required agro-climate data, including daily monthly and annual rainfall [65–68]. In addition, rainfall data were collected from CHIRPS/DAILY based on the (NMA) active station (Table 2) and these stations were exported to Google Earth engine to fill missing data gaps according to the agrometeorological station estimate is important [69] to fill data uncertainties. Few scientists who adapted hydrological research in Bilate watershed did not describe how

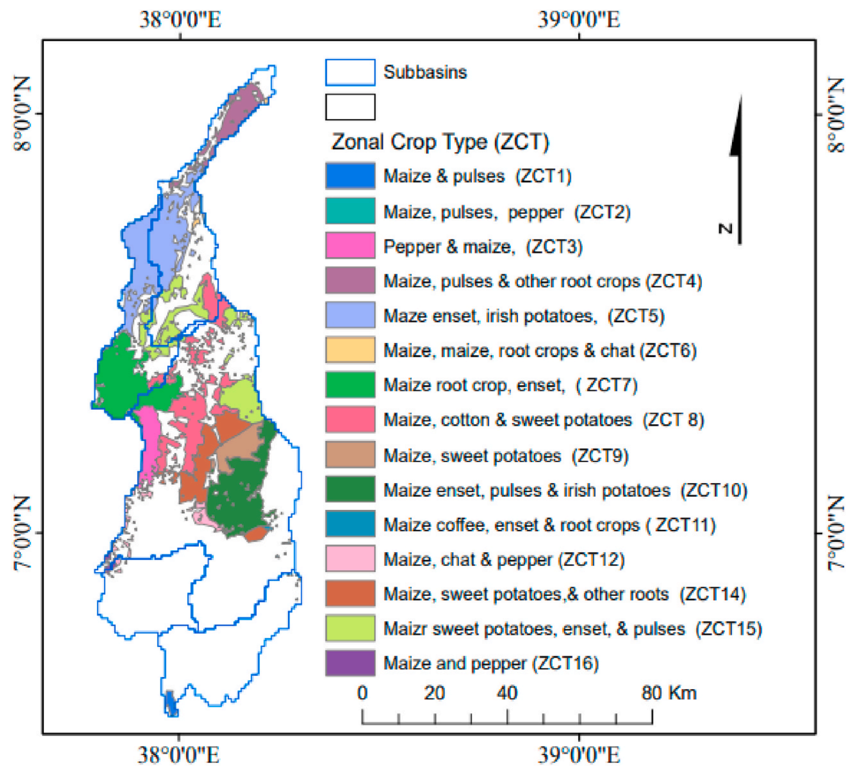

Fig. 2. Seasonal crop data classification.

Table 2
Climate data observation station based on Thiessen polygon weight factor Bilate down stream.

NMA_Station	Lat	Lon	Elv	Area_OP [Km]	Wt_Factor	Wt in %
Shone	7.134	37.953	1959	351.546	0.075	7.5
Aje	7.291	38.352	1846	152.309	0.032	3.5
Wulbareg	7.736	38.120	1992	512.729	0.129	12.9
Butajra	8.150	38.367	2000	101.341	0.022	2.2
Wolaita Sodo	6.850	37.750	1643	170.118	0.015	1.5
Durame	7.200	37.950	2000	208.691	0.044	4.4
Boditi School	6.954	37.955	2043	419.412	0.068	6.8
Bilatetena	6.917	38.117	1496	918.116	0.195	19.5
Bedessa	6.869	37.936	1609	205.532	0.065	6.5
Alaba Kulito	7.311	38.094	1772	870.844	0.185	18.5
Angacha	7.341	37.857	2317	388.421	0.082	8.2
Hosana	7.567	37.854	2307	510.097	0.108	10.8

the observation station was selected for climate data observation stations [70,71].

Since long-term averages of area precipitation distribution [66,67,72,73] play a larger role in modeling agricultural watershed characterization, precipitation proportionality for model input should be the region of uncertainty based on selected measured observations [74]. Therefore, the Thiessen polygon method is a good approach for gap minimization and its impact on predicting the water balance and water content of the plant root zone due to the uncertainty of rainfall measurement [75]. The Thiessen polygon technique sets a fixed weighting factor for the area coverage of a station, and the arithmetic average method assumes that the precipitation field is homogeneous [66]. Since the pattern of rainfall homogeneity in the study area was tested by other scientists [65]. It is possible to apply the Thiessen polygon technique [76] to select observation stations [67]. However, it has not been clarified how these scientists selected these stations and this research selected 12 stations (Fig. 3) using the Thiessen polygon method [77,78], which is based on the information from agro-metrological crop modeling concept for predicting the water balance estimation of crop root zone [64]. In addition to seven measured crop season observation stations, rainfall data were selected for model input as independent variables for predicting crop canopy content and observing growing zone water content.

Selected stations (Table 3) were selected based on their proximity to agricultural areas and availability of reliable and consistent data. The use of Thiessen polygons [68,79,80] allows estimation of plant root zone water balance, which is crucial for understanding and managing water resources in agricultural systems. By incorporating measured observation stations for rainfall data [81–85], the model can accurately predict crop stand contents and monitor water content in the growing zone, providing valuable insights for crop management and irrigation strategies.

3.4. Rainfall pattern

The average precipitation in the growing zone, which is crucial for plant growth during the observation season, falls predominantly in May and June. This time frame is selected for model calibration, which aims to predict plant canopy water content. Given the importance of rainfall windows for crop water uptake from the soil root zone [72], there is a strong correlation between comparing N nutrient uptake and estimating (NO_3^--N) leaching/runoff from cropland [73]. Therefore, accurate prediction of precipitation patterns in May and June is crucial for calibrating the model and accurately estimating plant canopy water content. Furthermore, studying precipitation windows for crop water uptake is essential for understanding nutrient uptake and potential leaching or runoff of (NO_3^--N) from cropland. This highlights the importance of this relationship. Rainfed agronomic practices followed by bimodal rainfall were applied to Bilat cropland (Fig. 4), and based on its rainfall pattern, data were collected to calibrate earth observations.

Accordingly, there are two growing seasons in the study area, namely the Belg growing season with long rainfall intensity and the Mahir growing season with short rainfall intensity [65]. This information is important to determine a specific season for nitrogen-N fertilizer leaching and occurrence of run-on losses in the farmland watershed, as it has significant impacts on the downstream areas [79]; therefore, the Belg season for the study area is sensitive to the calibration of model climate parameters. Accordingly, for the current study, monthly mean precipitation amounts from the period 1981–2020 are given for mid-March, April and May to the end of June. The dynamics of watershed characterization modeling could be greatly influenced by the selection of an agrometeorological observation station [86,75,66].

3.5. Missing data estimation

The missing data for precipitation observation are calculated using the daily CHIRPS observation by overlaying the longitude and latitude of the identified measured station points into daily, monthly and annual estimates using the Google Earth engine [87–91]. This effectively mitigates the effects of climate changes in crop water and nitrogen management in agricultural watersheds [67] This approach enables a more accurate and comprehensive understanding of rainfall patterns in specific agricultural watersheds and enables farmers to make informed decisions regarding irrigation and fertilization. By incorporating data from CHIRPS and using the Google Earth engine, researchers can fill in the gaps left by missing rainfall observations, providing a more complete picture of water availability for crops. Accurately observed rainfall data is crucial for adapting to the changing climate and ensuring sustainable

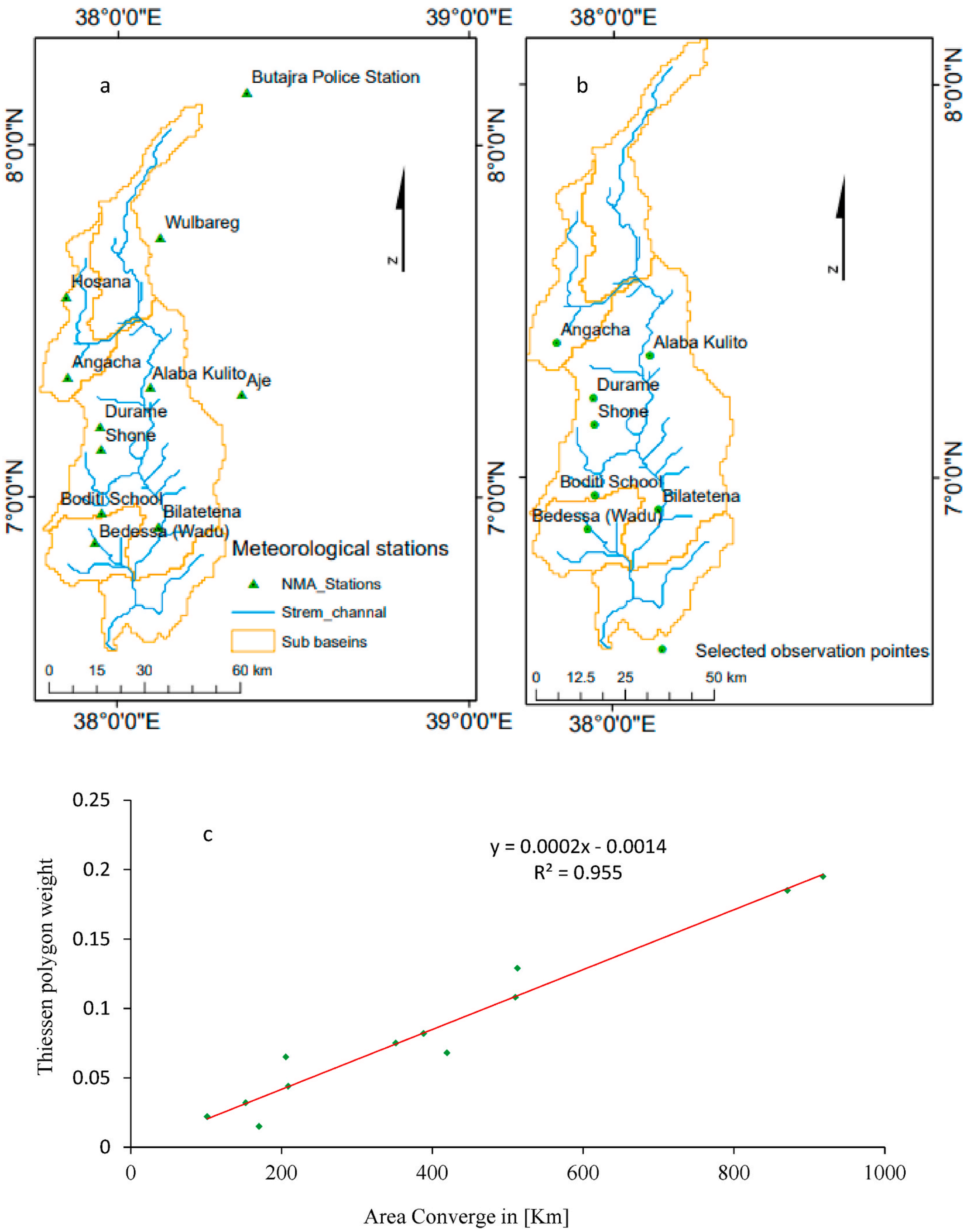

Fig. 3. (a) Active meteorological station, (b) Thiessen polygons for selection of data observation station and (c) correlation between Thiessen polygons weight vs Area Coverage.

agricultural practices in the face of increasing water scarcity [92,81]. Overall, integrating CHIRPS data improves the resilience and sustainability of agricultural systems in the face of a changing climate. Accordingly, we linked the water gauge observation station (Table 1) with Google Earth Engine to estimate the missing precipitation data from 1981 to 2020 to fill the gap in precipitation observation. Furthermore, CHIRPS data can be highly correlated with point data observation [82] when it comes to observing missing precipitation data. We used the collected daily baseline rainfall data for gap filling from each measured station for the year from 1981 to 2020 using the normal ratio method [93] based on the specific objective of the current study. Normal annual precipitation does not exceed 10% of the values considered in the selected gauge observation and we have validated this using statistical analysis results.

Table 3
Annual average rainfalls from CHIRPS and selected NMA gauged station.

Station name	Gauged St Ob RF [mm/year]	CHIRPS pt Obs RF [mm/year]
Wulbareg	1032.25	1014.25
Durrame	1204.28	1206.99
Boditi School	1293.44	1291.22
Bilate tena	999.47	1011.32
Badessa	1115.33	1173.20
Alaba Kuito	1040.23	1097.22
Hosana	1310.21	1324.33

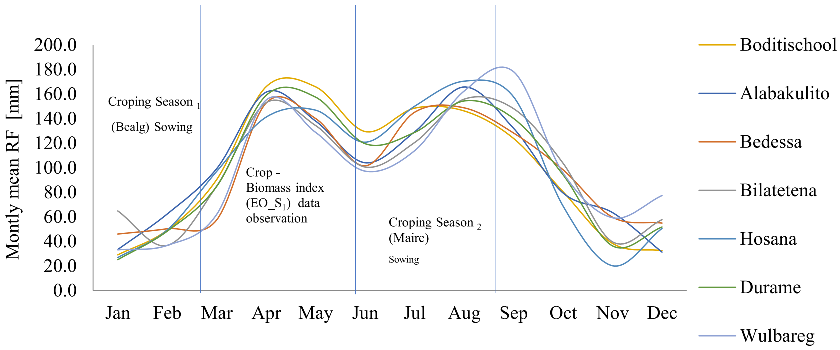

Fig. 4. Monthy mean rainfall distrbution of Bilate Farm land watershed for selacted gauged observation (1981–2020).

3.6. Accuracy assessment

The spatial and temporal distribution for precipitation observation is crucial for simulating hydrological models at the watershed scale [83], but it is challenging to select the right observation station based on the degree of influence on achieving research objectives. And based on the working principle of Thiessen polygon [65], an Arc-GIS simulated [18] for the influencing measured station is selected for model calibration since the precipitation homogeneity test of Bilate watershed was carried out by other scientists [67] for their research objective. According to the information provided, 12 active meteorological data observation stations (Fig. 3a) are identified for model-calibrated precipitation observation based on the specific objective of the current study. Selecting a measured precipitation observation station based on its area coverage is important for the accuracy of predicting crop water balance. Therefore, the rainfall data observation was identified (Table 2, and Fig. 3b).

Since the coverage of precipitation distribution over a given catchment depends on the weighting factor of a measured observation station in a polygon, it can be correlated [88] so that the acceptance of selected stations below is correlated (Fig. 3c) to validate the model inputs. As one of the most sensitive independent climate variables for plant parametric analysis of nitrogen runoff and leaching [84], identification of precipitation observation stations is important. In this regard, the validated precipitation observation station identified by the Thiessen polygon method proves suitable for this research-specific objective. Its correlated coefficient for liner regression was found ($R^2 \geq 0.5$ and $P \leq 0.001$). Since precipitation is one of the most important hydrological components for nitrogen modeling in agricultural watersheds [76], a measured precipitation observation station should have been carefully identified based on the research objective. Seven precipitation observation stations were also selected. The selected observed rainfall from the observation station is rainfall from twelve stations for the total threshold of the Bilate watershed (Alaba, Bilatena, Boditischool, Badesa, Durame Hosana and Wulbareg). Based on the specific objective of the current study, the normal annual precipitation does not exceed (10%) the value considered in the selected gauge observation and was validated by static analysis results as given in equation (1):

$$V_o = \frac{\sum_{i=1}^{n} wi * Vi}{\sum_{i=1}^{n} Wi} \tag{1}$$

where; W_i is the weight of the ith nearest climate station. Vi is the observational data of the ith nearest climate station and weights for the surrounding stations used in the estimation [85] are calculated as given in equation (2):

$$\mathrm{Wi} = [\mathrm{R}^2\left(\frac{\mathrm{Ni}-2}{1-\mathrm{R}^2}\right)] \tag{2}$$

Where R is the correlation coefficient between the target station of the NMA station for missing data and the ith surrounding station for collected observation, NMA is the National Metrological Gauged station used for the missing data station and the ith surrounding station for collecting point observation from CHIRPS/DAILY, [42,80,82,93] and Ni is the number of station points used to derive the correlation coefficient, and after all missing data has been computed, the following annual average rainfall is used for model input calibration (Table 2 and Fig. 3c). The comparison result for CHIRPS observation and used NMA gauged station, was liner correlated for validation and correlation coefficient (r) reflected relationship between two observation result for validation was scored (95%) of confidence interval, with moderate correlation value $0.5 <$ for $(R^2) = 0.95$ and $P < 0.001$ (Table 4) between the two observations [94] the absolute value of $|r|$ in the (equation (3)) has indicted a strong correlation $(0.9 < |r| \leqslant 1)$.

$$(r) = \frac{\sum_{i=1}^{n}(Xi - Xav)(Yi - Yav)}{\sqrt{\sum_{i=1}^{n}(Xi - Xav)^2 \sum_{i=1}^{n}(Yi - Yav)^2}} \tag{3}$$

Y is the mean rainfall and the mean of SSNMA (Selected Station of National Meteorology Agency), respectively during the studied periods. Where r is the correlation coefficient, n is the length of the time series, and i is the number of years during analyzed periods (1981–2020) X_i and Y_i are the rainfall and SSNMA in the year ith Year of observation.; Model preparation.

Based on the spatial heterogeneity of crops in the study area, the Geographically Weighted Rogation (GWR) model uses the conventional regression approach and emphasizes the need to set different parameters for the same explanatory variables [95]. The Geographically Weighted Rogation (GWR) model also proves to be appropriate in relation to the conceptual model of this study, based on an understanding of the model limitations and strengths for scientists in making decisions about cultural dynamics in the watershed. Regarding the conceptual model of this study, the Geographically Weighted Rogation (GWR) model is suitable [95,96]. Therefore, simulation of cropland zone statistics from the MODIS 250 m [49,52,57,97] improved the response of the vegetation index for each specific crop type for crop water balance based on the average precipitation (aRF) for the classified cropland area. It also predicts plant canopy water content as an indicator of nitrogen leaching or runoff from cropland watersheds. Due to the heterogeneity of crop parameters [47], the GWR model was prepared for use in the current study, and the relationships between the area-observed average seasonal precipitation variables of the growing zone can be highly correlated to predict the crop canopy water content. The GWR model takes into account the spatial variability of rainfall in different growing areas, enabling more precise estimates of water balance. By incorporating the average seasonal precipitation variables of the growing zone, the model was able to accurately predict plant canopy water content. This information is critical for assessing the risk of nitrogen leaching or runoff in the cropland watershed as it provides an indication of the amount of water available for plant uptake and the potential for nutrient loss. In addition, the model can also help determine the optimal irrigation schedule for different growing areas, ensuring that plants receive sufficient water without overusing it. This can contribute to more sustainable water management practices and higher crop productivity.

Table 4
Statistics summery for validation missing data estimation.

Regression						
Regression Model	Linear					
LINEST raw output						
0.95	74.07					
0.10	114.05					
0.95	31.18					
91.61	5.00					
89035.57	4859.59					
Regression Statistics						
R^2	0.94					
Standard Error	31.17					
Count of X variables	1					
Observations	7					
Adjusted R^2	0.93					
Analysis of Variance (ANOVA)						
	Df	SS	MS	F	Significance F	
Regression	1	89035.57	89035.57	91.60	0.00021	
Residual	5	4859.59	971.91			
Total	6	93895.16				
Confidence	0.95					
	Coefficients	Standard Error	t-Statistic	P-value	Lower 95%	Upper 95%
Intercept	74.07	114.04618	0.64	0.54467	−219.09	367.23
Gauged St Obs	**0.95**	0.09	9.57	0.00021	0.69	1.20

Gauged St Obs	Predicted	CHIRPS Obs	Residual	Station name
1032.25	1055.30	1014.25	−41.05	Wulbareg
1204.28	1218.83	1206.99	−11.84	Durrame
1293.44	1303.58	1291.22	−12.36	Boditi School
999.47	1024.14	1011.32	−12.82	Bilate tena
1115.33	1134.27	1173.2	38.93	Badessa
1040.23	1062.89	1097.22	34.33	Alaba Kuito
1310.21	1319.52	1324.33	4.81	Hosana

4. Data analysis

Seasonal precipitation is based on measured observations (Table 3 and Fig. 4) of rainwater entering the growing zone. The useful water consumption from precipitation is estimated for the classified cultivation zone (Fig. 2) in [mm/ha/month] as the rate of precipitation water entering the cultivation zone per unit of arable land [32,98]. Therefore, classified cropland is used to calculate the amount of precipitation that falls on a unit of cropland each month and is expressed in millimetres per hectare (equation (4)). Additionally, these data were used to calibrate the model and estimate the amount of nitrate that transported soil particles out of the root zone. This helps to track and understand the effects of nitrate contamination on surface and groundwater recharge using the seasonal water balance of crops.

$$\begin{array}{l}\text{Water in croping zone for sesonal} \\ \text{observation} = \dfrac{\textit{Croping season Mean rainfall in mm}}{\text{Classified cropping zone}}\end{array} \tag{4}$$

Plant canopy water content can be predicted from the reflectance of the plant-enhanced vegetation index of MODIS 250 m EVI for each image pixel value of the cropland [21]. The principle of geographically weighted regression modeling (GWR) for predicting [95,89,99,100] crop water balance based on crop growth curve for crop heterogeneity as model parameter calibration [101] proved to be conceptually important. In this concept, crop data is considered as model input and its extension of OLS (Ordinary Least Squares) regression allows to consider locally varying parameters as spatial instability in a sample and the stochastic working principle of the (GWR) model [102] as follows in the (equation (5)).

$$y_i = \beta_o(U_i, V_i) + \sum_{i=1}^{P} \beta_k(U_i, V_i)X_{ik} + \varepsilon_{\mathrm{i}} \tag{5}$$

Where; y_i is the dependent variable (EVI mean from crop zonal statics with respect to average cropping land rainfall for cropping season), Zone ith crop type for (U_i V_I) is the geo spatial location of crop i, β_0 (U_i, V_i) is the intercept at location ith β_k (U_i, V_i) which is the local parameter estimator for independent variable (X_{ik}) at location ith, crop EVI mean for the (ε_i) of the error term with this the model simulated from the shape area in (ha) from cropland and the equation employed for crop water balance is as follow in (equation (6)).

$$y_i = \beta_o(A_i) + \sum_{i=1}^{P} \beta_k(A_i)X_{ik} + \varepsilon_{\mathrm{i}}.. \tag{6}$$

Where; A_i is the shape area of (*i*th) crop land, to predict the regression coefficients based on a distance-decay function (W_{ij}) in (equation (7)) and it is applied as a distance weighting factor between a modeled location and the observations [103]. When the sample points are irregularly distributed, a variable bandwidth increases, which increases the consistency of the model productivity formula through an adaptive weighted kernel [102]. Based on the concept of crop heterogeneity for its stochastic principle.

$$\mathrm{W_{ij}} = \begin{cases} \left(1 - \left(\dfrac{dij}{\Theta ij(k)2}\right)2 \quad \text{for } \Theta i(k) \ > \ \Theta i(k) \right. \\ 0 \; dij > \Theta i(k) \end{cases} \tag{7}$$

where (d_{ij}) is the distance between observations i and j, θ_i (k) is the adaptive bandwidth defined by the (kth) nearest neighbor distance. For a case in which the distance between observations is greater than the adaptive EVI pixel width, the distance decay function becomes zero [102]. And annual cropping season of each year time series from (2001 up 2020) crop water balance is predicted in GWR model with liner regression ($R^2 \geq 0.5$) simulated and see model prototype.

5. Result and discussion

5.1. Calibration and validation

The result of the geographically weighted regression (GWR) model simulation [104,105] with (EO-MODIS 250 m NDVI/EVI) [22] of the extracted time series arable land is converted into the land class (MODIS-MCD12Q1) of the International Geosphere-Biosphere Program (IGBP) [52,54,97] which integrates value (12). This is used to estimate the crop water balance of the identified main water balance of rain-fed crops (Fig. 11) based on the rainfall pattern indicator of the study area as an indication of cropland runoff/leaching (NO_3^--N). The calibration of the GWR model is carried out based on an AICc method for observed average precipitation in terms of goodness of fit to the predicted crop water balance, based on the concept of spatial or crop data heterogeneity [103].

The pixel of cropland EVI has predicted crop water canopy water content in GWR model with correlation coefficient ($R^2 \geq 0.5, P < 0.001$) and this interval is satisfactory to accept result [106]. Time series (NO_3^--N) runoff\leaching quantification is extremely complex to hydrological model [107]. Because it is very sensitive to the observation of model inputs in space-time, depending on parameters and variable factors such as crop dates and soil physicochemical properties [45]. However, it is difficult to obtain time series data as for the study area. Due to this complexity and the lack of time series observation data in the study area, this study rather aims to use an empirical model (GWR) to predict plant seasonal water use efficiency and plant canopy content [108], observed time series nitrate data uncertainty for modeling contamination at regional scale for Bilate agricultural watershed has great role in research model preparation also crop heterogeneity is important parameter to (NO_3^--N) runoff\leaching estimation [103]. Estimating cropland (NO_3^--N) runoff \leaching is also extremely associated with crop water balance for the intensity of crop root zone rainfall induced water content in cropping land [109]. *The simulated model outcome of crop water balance and observed root zone soil water content of cropping zone for wet season in the study area indicates calibrated model outcome.* Predicted (CCWC) and observed (Z_SWC) results, the root mean squared error (RMSE) < 0.5) and liner correlation ($R^2 \geq 0.5$) of (95%) is validate the result for confidence interval for model outcome and correlation coefficient (R^2) as in (equation (8)) and RMSE in (equation (9)):

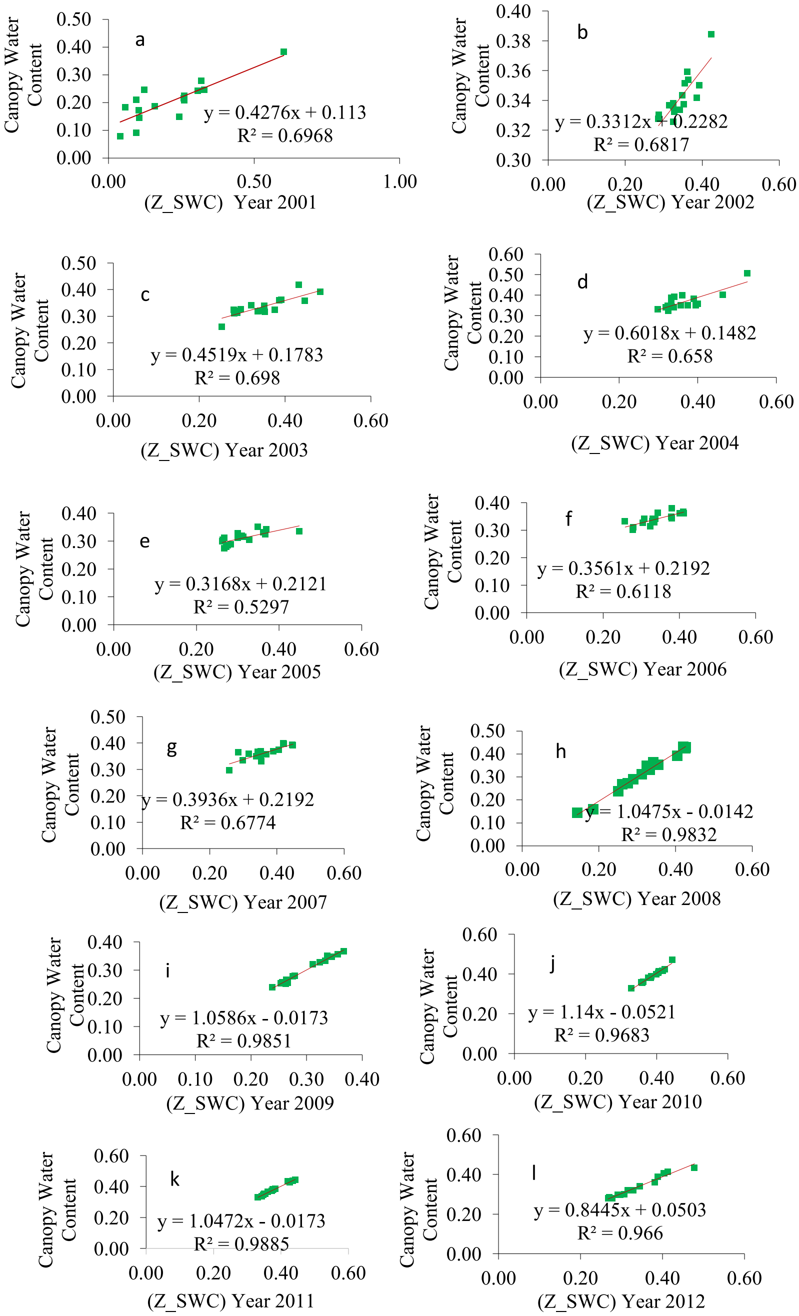

Fig. 5. Predicted canopy water content vs soil water content (Z_SWC) for observed cropping in the year 2001 (a), 2002 (b), 2003 (c), 2004 (d), 2005 (e), 2006 (f), 2007 (g), 2008 (h), 2009 (i), 2010 (j), 2011 (k), 2012 (l), 2013 (m), 2014 (n), 2015 (o), 2016 (p), 2017 (q), 2018 (r), 2019 (s) and 2020 (t).

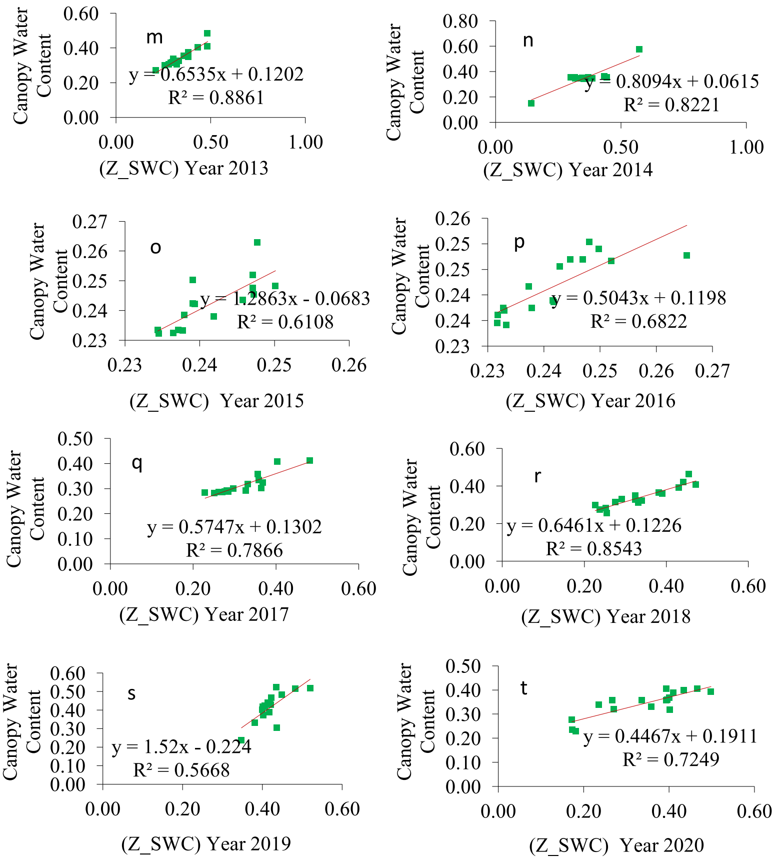

Fig. 5. (*continued*).

$$R^2 = \sqrt{\frac{\sum_{i=1}^{n} (OZ_{SWCi} - P_{CWCi})^2}{\sum_{i=1}^{n} \Big(}} \tag{8}$$

Root mean square error

$$RMSE = \sqrt{\frac{\sum_{i}^{n} (PCWC_i\text{-}OZSWC_i)^2}{N}} \tag{9}$$

where N is the total number of observations for monthly average precipitation [mm/month] of the model input for root zone soil water content per crop area in a crop type. (PCWCi) is the model predicted value of culture water balance per crop type. And (OZSWCi) is the observed soil water content of the plant root zone for each crop species. The output of the GWR model is used in addition to the R^2 acceptance range and ANOVA statistical approaches to validate the model (Fig. 5a to Fig. 5t) and tested with the specified correlation coefficient ($R^2 \geq 0.5$ and $P < 0.001$) for each year of simulation.

5.2. Crop biomass

The calculation of the cropland zone statistics for the biomass index using the EVI was calculated in the Arc GIS raster calculator [69,70,110,111] on the MODIS image using the following equation. Based on the cropland trough, the extraction by attributes from the cropland class value of (12) from the MODIS-IGBP land cover type [112] was converted into a shape file for cutting crop data from national livelily hood data, based on and validated through field survey data for soil truth crop information [113] MODIS/Aqua [57] Enhanced Vegetation Indices (EVI) time series [64,69,114] indicate improved agricultural information such as: B. the food security index due to nitrogen degradation of farmland [115]. Statistics for the biomass index are calibrated to the model simulation followed by sample precipitation (Fig. 6) for the 16-day L3 Global 250 m SIN Grid V061 data observation using (equation (10)).

$$Crop\ land\ EVI = G\frac{NIR - RED}{NIR + C1 * RED - C2 * BLUE + L} \tag{10}$$

where NIR (near infrared), red and blue are the full or seasonal atmospheric corrected surface reflectance (for Rayleigh scattering and ozone absorption) [116,117]. L is the canopy background adjustment to correct for nonlinear differential NIR. C1 and C2 are the coefficients of the aerosol resistance term. The blue band is used to correct aerosol influences in the red band. G (2.5) May be cropland, is a scaling factor for plant growth in the rainy season and the coefficients used for MODIS EVI [114] algorithm are $L = 1$, $C1 = 6$, $C2 = 7.5$ and $G = 2.5$ [118]. The biomass statistics of the growing zones are calculated based on the average rainfall of the growing season of the classified growing areas. Since the water balance of crop plants depends on the amount of water that reaches the root zone through precipitation [20], as an independent variable in the modeling simulation on cropland EVI (Fig. 6a–b, Fig. 6c and d), which is dependent variable for the arable land zone statistics [119]. Using this principle, it may be possible to predict plant canopy water and observe soil water content in the root zone of crops [108,112]. As a result, cropland zone statistics were c reated, which were used to link the cropland shape file to classified croplands. Rainy season cropland zonal biomass statistics of major crops in the study area (Fig. 7) are below an acceptable range for growth range for all crops [120,121]. The growth curve [30] for the uncertainty interval of the rainy season beginning/maximum/end ($0.25 \leq$ /crop zone EVI≤ 0.75) [33]. In addition, the result EVI ≤ 0.25 can be an.

indicator of the mineral degradation index of the farmland in the rainy season [109,113]. With this result, harvest data from EVI for the study area were integrated into the model [113,122] to predict the water content of the plant canopy.

5.3. Canopy water content

The crop canopy water intercept (in mm/day) for observed root zone water in (%) (Figs. 8 and 9) can be an indicator of the water use efficiency of the plants based on the intensity of rainfall in the entire growing zone [106]. The regionalization of cropland, followed by pattern rainfall, depends on the reflection of the cropland vegetation index in the growing season of crops [123,118] and depends on

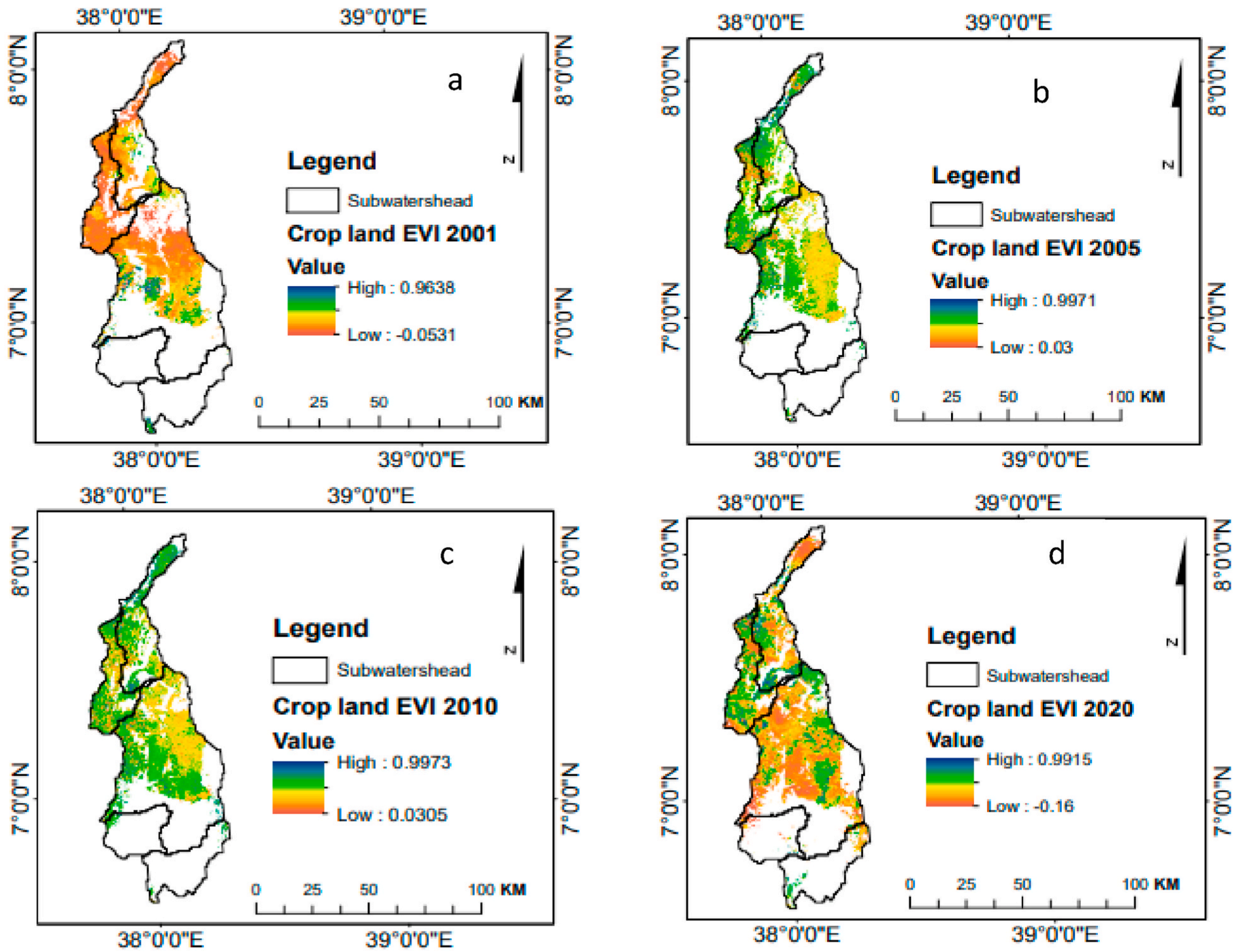

Fig. 6. Cropland EVI for simulation of cropping zone statistics prototype for the Year 2001 (a), 2005 (b), 2010 (c) and 2020 (d).

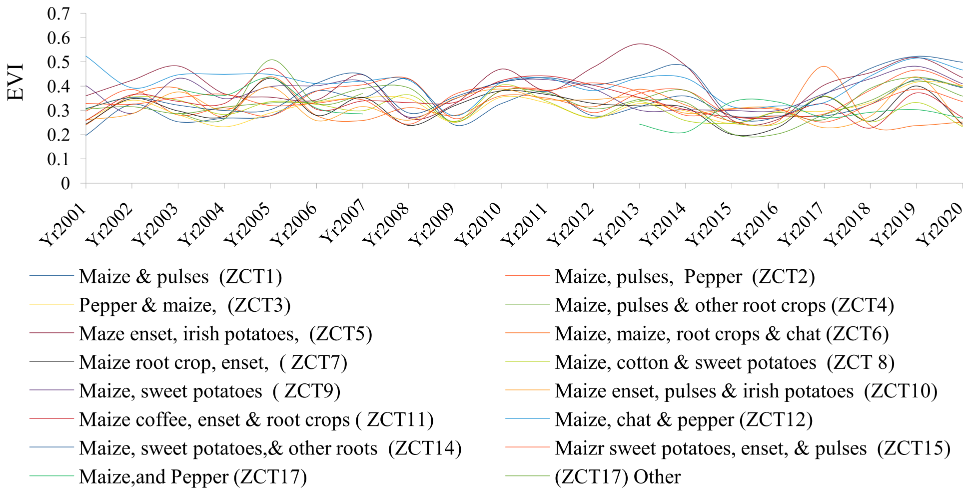

Fig. 7. Zonal crop biomass statistics of managed mineral soil index.

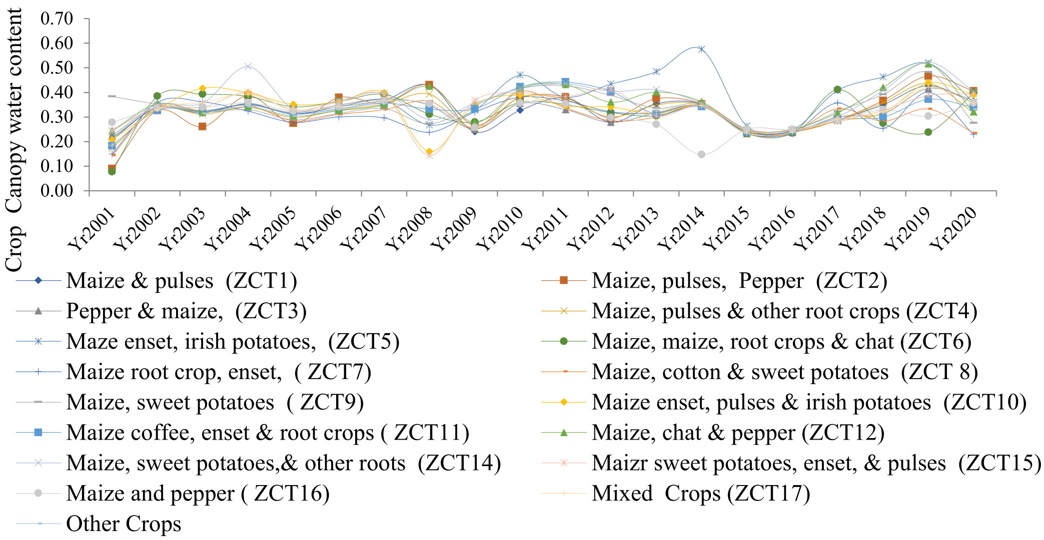

Fig. 8. Predicted crop canopy water content.

the rainfall intensity in the growing zone. When the continuous precipitation rate is lower than the water content of the tree canopy, the captured water is not sufficient to meet the atmospheric demand within a time step [124]. This means that the estimated crown water content is used as an indicator of (NO_3^--N) runoff/leaching from cropland and is dependent on the observed soil water content in the root zone (RZ_SWC) based on the growing season rainfall [125,126]. And the total annual crop water balance by liner regression for model calibration with the observed water content of the crop root zone in the rainy season.

Based on the result of the seasonal change of root zone storage, the water balance is estimated for the (NO_3^--N) index for precipitation or (RZ_SWC) for the seasonal crop over the water content of the plant canopy. The conceptual model satisfies possible (NO_3^--N) leaching\rUnoff index [123,126]. This means that nitrogen fertilizer leached or leached due to the water content of the soil is greater than in the growing zone. The water holding capacity of the soil is greater, which results in the water draining below the root zone of the plant [127] and the transport of nitrogen nitrate from the root of the plant is accelerated. Zone in which a soluble form of nitrate (NO_3^--N) enters the groundwater. It can also lead to nitrate contamination of groundwater. Since the state of the water balance of crops depends entirely on the water content of the soil due to the amount of precipitation on the cultivated area [128,129], the runoff/leaching of (NO_3^--N) reacts strongly to the precipitation [127,130,131] during the harvest season and the probability of groundwater recharge high water content of the soil in the root zone leading to contamination.

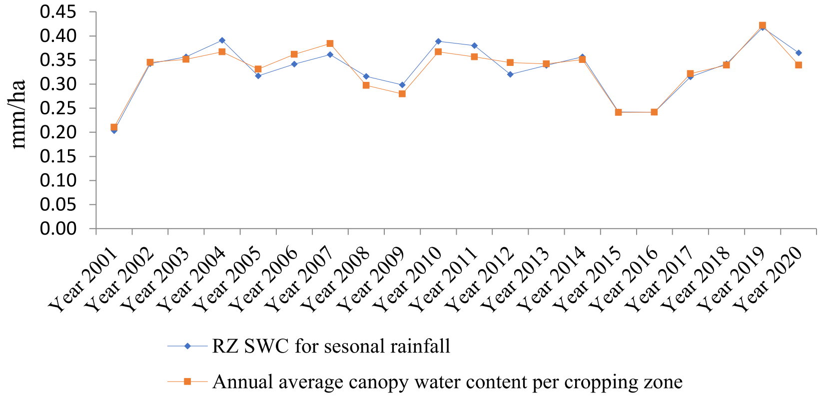

Fig. 9. Canopy water content and seasonal root zone water content for indictor of surface and groundwater nitrate contamination index.

5.4. *Leaching runoff index*

As the water content in the root zone of crops decreases, water is held more tightly to mineral surfaces. However, in other words, this means that the result can be interpreted for the water balance interval (0 to −0.033) of the plant root zone (Fig. 10), showing an increase in the soil drainable state of (NO_3^--N). A higher leaching runoff index indicates [120,121,132] that more water is lost through runoff, which can lead to nutrient pollution and reduced water availability for crops [26–28]. Therefore, increased soil drainability (NO_3^--N) suggests that there is an increased risk of leaching and nutrient loss in the root zone of crops. This can have negative impacts on plant growth and yield, as well as the overall health of the ecosystem. Additionally, excessive leaching and nutrient losses can contribute to water pollution [66,75,133,134] in nearby bodies of water. It is critical for farmers and land managers [135–137] to implement appropriate irrigation and nutrient management practices to minimize these risks and ensure sustainable crop production.

nitrate contamination.

This means that the fertilizer's nitrogen cycles between plant nitrogen uptake and soil nitrogen mineralization [12,13,138], with the primary removal process of (NO_3^--N) runoff and leaching into surface or groundwater. This can lead to reduced crop productivity and nutrient availability, as well as possible contamination of water resources. To mitigate these problems, farmers may need to implement strategies such as precise nitrogen application and improved irrigation management to minimize leaching losses [5,6,16]. Additionally, regular soil testing and monitoring can help determine crop nutrient needs and manage fertilizer application to ensure optimal nutrient cycling and minimize environmental impact. Overall, controlling water balance and nutrient cycling in arable land is crucial for sustainable agriculture and protecting water quality in (equation (11)).

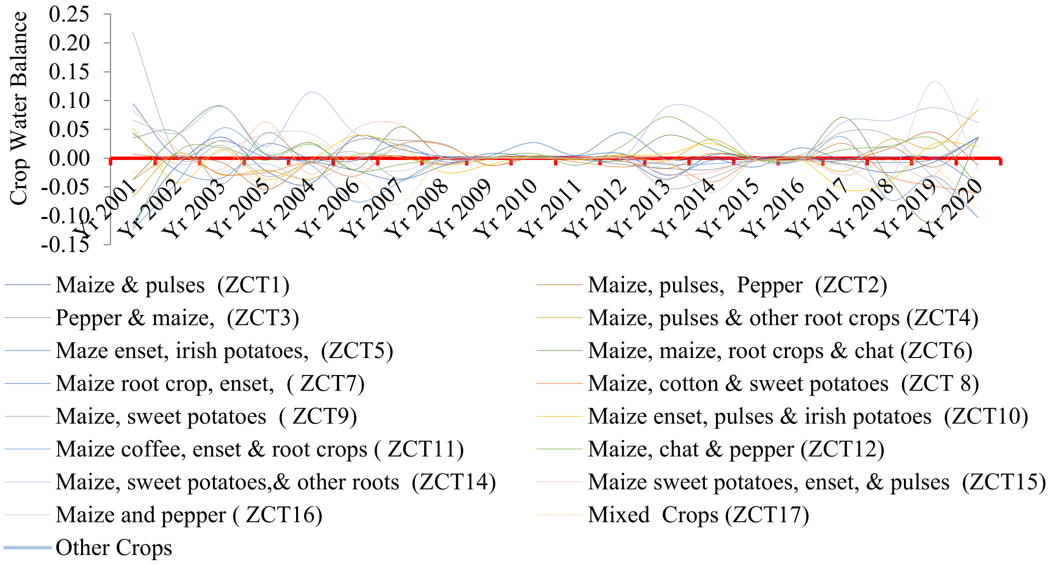

Fig. 10. Crop water balance by crop type.

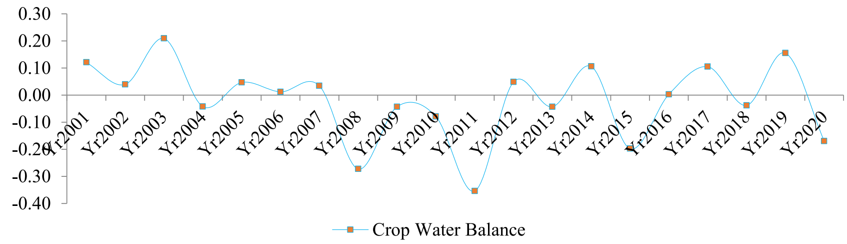

Fig. 11. Time series (2001–2020) crop water Balance for nitrate runoff\leaching index.

$$\text{Nitrate Runoff} \setminus \text{leaching index can be} = \left[0.5 \geq \frac{\text{CCWC}}{RZ\_SWC} \geq 1\right] \tag{11}$$

where CCWC is the water content of the crop canopy for the monthly average rainfall of the crop season in mm and RZ_SWC is the observed soil water content of the crop root zone for classified cropland sampled from African soil grids. Root depth data [139,140] observation for the average root zone depth was 30 cm–50 cm for seasonal N input in kgNha-1 year-1. The annual average water content of the tree canopy of the growing areas (Fig. 9) is used to calculate the seasonal water balance of the crops (Fig. 10). For SWC it is greater than or equal to the water content of the tree canopy which shows the (NO_3^--N) contamination index. Accordingly (2004, 2008, 2009, 2010, 2011, 2013, 2014, 2015, 2018 and 2020) seasonal nitrate leaching and runoff from the growing zone were indexed. Water use efficiency (WUE) is highly correlated with crop nitrogen balance (NUB). The estimate of (NUE) [47] correlates with the annually calculated summary for (WUE) of this specific work, see (Supplement Figs. 12 and 13). And the annual water use efficiency and crop nitrogen balance time series (2001–2020) are related based on validated and tested simulation results (Fig. 5) to further confirm the model simulation results. The conceptual model is consistent for the period when precipitation is higher than CCWC. The calculation of (NO_3^--N) runoff/leaching is expected to be based on the precipitation climate indicator [141]. The (SWC) ratio to root zone results are summarized (Table 5) to compare the plant root zone nitrogen balance estimated in the previous specific objective of this research.

5.5. *Crop water balance*

The seasonal crop water balance calculated using (equation (12)) below indicates the potential for runoff/leaching of nitrate in the groundwater system below the root zone [112].

$$\Delta S = \sum_{i}^{n} (O_{swc} - P_{cwc}) \tag{12}$$

Table 5
Time series Crop Water and Nitrogen Use Efficiency for Crop land N runoff \leaching indicator.

Year	Observed Volumetric zonal SWC [%] per R depth	Predicted Zonal Canopy Water Content	Crop Nitrogen Balance	Crop Water Balance	Crop Nitrogen Use Efficiency	Crop Water Use Efficiency
2001	3.369	3.248	0.121	0.1208	0.964	0.994
2002	5.519	5.479	0.072	0.0395	0.991	0.993
2003	5.912	5.703	0.142	0.2091	0.985	0.983
2004	6.209	6.255	−0.016	−0.0423	1.002	1.011
2005	5.339	5.297	0.021	0.0467	0.997	0.984
2006	5.790	5.788	0.147	0.0120	0.985	0.983
2007	6.150	6.147	0.282	0.0341	0.969	0.992
2008	4.742	4.755	−0.189	−0.273	1.027	1.019
2009	4.474	4.476	−0.066	−0.043	1.009	1.000
2010	5.834	5.869	−0.082	−0.079	1.006	1.001
2011	5.698	5.707	−0.206	−0.854	1.025	1.017
2012	5.167	5.119	0.120	0.0485	0.984	0.991
2013	5.427	5.470	−0.073	−0.0431	1.009	1.017
2014	5.709	5.614	0.034	0.1056	0.996	0.996
2015	3.863	3.875	−0.041	−0.498	1.005	1.001
2016	3.871	3.868	0.083	0.0029	0.990	0.997
2017	5.146	5.041	0.099	0.1049	0.989	0.990
2018	5.435	5.473	−0.014	−0.0381	1.002	1.000
2019	6.752	6.678	0.144	0.1551	0.956	0.996
2020	5.792	5.835	−0.157	−0.1697	1.019	1.001

Where; ΔS is the Change in water storage for crop root zone and O_{swc} is seasonal observed soil water content for average root depth of ith year for main crops type in the study area. And P_{cwc} is seasonal predicted crop water balance of ith year for main crops type in the study area. The crop water balance estimates are based on the predicted seasonal observed root zone soil water content and canopy water content [142,143]. Therefore, crop water balance [144–146] assessment along with the Cropland (NO_3^--N) runoff/leaching index is crucial to understand nitrate contamination assessment (NO_3^--N) in groundwater [147] since runoff/leaching occurs when rainfall or root zone soil water content surpasses the crop water balance. Crop Nitrogen Use Efficiency (CNUE) and Crop Canopy Water Content (CCWC) equilibrium are correlated with soil water content shows that nitrogen input variations. The positive difference between observed and predicted values indicates potential (NO_3^--N) runoff/leaching and a negative cropland water and nitrogen balance suggests crop stress. Increased rainfall corresponds to higher surface runoff and nitrate interflow [148,149]. Since surface and groundwater nitrate contamination modeling is completely dependent and sensitive to the amount of rainfall induced in surface area. Accordingly, the soil water content observed form seasonal cropping zone rainfall [149–152] (Fig. 11) is indicating the estimation of crop water balance for the cropland (NO_3^--N) rainfall induced leaching\runoff index [153]. Therefore, the rainfall intensity during cropping season is important to quantify volumetric cropping zone soil water content (see Supplementary Table 1) which predicts crop canopy water content. Annual seasonal crop water balance indicates the potential runoff \leaching of water and nitrate contamination flow above and below root zone [112].

6. Discussion

Indeed, hydrological modeling relies heavily on data, and the difficulty of obtaining time-series nitrate measurements for large watersheds represents a significant challenge [154–156]. The use of the geographically weighted regression (GWR) model approach [32,96,98,157,158] demonstrates to address this challenge by providing a tool for predicting nitrogen cycling in the cropland. This approach takes into account into various factors such as plant N uptake, (NO_3^--N) from plant root zone leaching, surface runoff and trends in nitrogen release. This comprehensive approach enables more accurate simulation of nitrate pollution in groundwater and surface water. The specific inclusion of crop-specific growing seasons in the GWR model takes into account the temporal variability of agricultural practices and emphasizes that different crops can have different effects on the nitrogen cycle [53,62,63,159]. This seasonal calibration adds a higher level precision to the model parameters and reflects the dynamic nature of agricultural systems. Precipitation variability is highlighted as a key factor affecting nitrate pollution in agricultural watersheds. Therefore, this study likely presents visual representations of how different precipitation patterns affect the transport of nitrates within the watershed using Figs. 3, 4 and 9. Understanding these patterns is dire for predicting and managing nitrate pollution since rainfall can affect the movement of nutrients through soil and into waterways [160]. Consequently, this study is suggesting understanding routine water quality monitoring is a proactive measurement needed. Regular water quality assessment enables timely detection of water quality problems and enables intervention before widespread occurrence of contamination. This preventive approach is essential to protect the environment and human health using acquisition of remote sensing data. Remote sensing technologies can provide valuable information about land cover changes, vegetation health and other relevant parameters over large spatial scales. Integrating such data into hydrological models increases their accuracy and provides a broader overview of the factors affecting nitrate pollution in large watersheds. In summary, the study uses the GWR model to address the challenges of limited nitrate measurements in large watersheds is valuable approach to understand surface and groundwater contamination. It highlights the importance of considering various factors in the nitrogen cycle, emphasizes the role of precipitation variability and routine monitoring of water quality which proposes the integration of remote sensing data to improve hydrological modeling in agricultural watersheds. This is better helping to understand the complex interactions between the nitrogen cycle and the water cycle in the watershed.

6.1. Limitations of the study

Nitrates can get into surface and groundwater from many sources. However, this study considers the agricultural practices as the main contributor to nitrate pollution and other factors are normal in the watershed. Additionally, the geographically weighted regression model may have limitations to represent the hydrological processes. Therefore, the findings could be used for developing strategies to manage nitrate pollution problems in the watershed in consideration of other factors are normal.

7. Conclusion

According to the results of this study, canopy water content below zero could indicate potential crop water shortages and indicates drought conditions. This finding is important for farmers and agricultural professionals as it can help them to monitor and manage water resources more effectively. Through regular measuring the canopy water content, farmers can make informed decisions about irrigation schedules and water allocation and ultimately improve crop yields and water use efficiency. Furthermore, this study highlights the importance of implementing sustainable agricultural practices to mitigate the effects of drought and ensure food security in the face of climate change. Deficits during the years (2004, 2008, 2009, 2010, 2011, 2013, 2014, 2015, 2018 and 2020) indicated nitrogen and water deficits for cultivation with nitrogen and water deficits in the rainy season which further confirm the results based on the water use efficiency of the crop. To follow up the result, the results of this study on the nitrogen balance of crops were used. Consequently, the potential N uptake was calculated in the years (2004, 2008, 2009, 2010, 2011, 2013, 2015, 2018 and 2020) for the total nitrogen applied in the root zone in [$Nkgha^{-1}$ yr^{-1}] and other growing years. The negative crop water and nitrogen balance shows that the results of the current study suggested possible (NO_3^--N), leaching\runoff from cropping zone. The quantities separated from arable land were released into the waterways in the identified years. It is therefore possible to link the crop water balance with crop nitrogen balance. This information is also important for tracking the sustainability of water, soil and environmental management as well as the impact of N fertilizer management on a cropland.

Ethics approval and consent to participate

An ethics statement is not applicable because this study is based exclusively on published literature.

Funding

This research received no external funding.

Availability of data

The data will be made available on request for the corresponding author *"Bereket Geberselassie Assa"*, upon reasonable request.

CRediT authorship contribution statement

Bereket Geberselassie Assa: Writing – review & editing, Writing – original draft, Visualization, Validation, Software, Methodology, Formal analysis, Data curation, Conceptualization. **Anirudh Bhowmick:** Writing – review & editing, Writing – original draft, Validation, Supervision, Methodology, Formal analysis. **Bisrat Elias Cholo:** Writing – review & editing, Writing – original draft, Validation, Supervision, Software, Methodology, Formal analysis.

Declaration of competing interest

The authors declare that they have no known competing financial interests or personal relationships that could have appeared to influence the work reported in this paper.

Acknowledgments

We appreciate the Arba Minch University Water Resource Research Center's financial and material support for the data collecting of the current study.

Appendix A. Supplementary data

Supplementary data to this article can be found online at https://doi.org/10.1016/j.heliyon.2024.e26717.

References

[1] FAO, The State of the World's Land and Water Resources: Managing Systems at Risk, 2011 [Online]. Available: http://www.fao.org/3/i1688e/i1688e.pdf.
[2] I.V. Muralikrishna, V. Manickam, Natural resource management and biodiversity conservation, Environ. Manag. (2017) 23–35, https://doi.org/10.1016/b978-0-12-811989-1.00003-8.
[3] M. Jarraud, A. Steiner, Summary for policymakers 9781107025 (2012), https://doi.org/10.1017/CBO9781139177245.003.
[4] J. Penuelas, F. Coello, J. Sardans, A better use of fertilizers is needed for global food security and environmental sustainability, Agric. Food Secur. 12 (1) (2023) 1–9, https://doi.org/10.1186/s40066-023-00409-5.
[5] D. Wang, et al., Effects of nitrogen fertilizer and water management practices on nitrogen leaching from a typical open field used for vegetable planting in northern China, Agric. Water Manag. 213 (June 2018) (2019) 913–921, https://doi.org/10.1016/j.agwat.2018.12.015.
[6] M.A. Elrashidi, et al., Loss of nitrate-nitrogen by runoff and leaching for agricultural watersheds, Soil Sci. 170 (12) (2005) 969–984, https://doi.org/10.1097/01.ss.0000187353.24364.a8.
[7] A.F. Bouwman, G. Van Brecht, K.W. Van Der Hoek, Global and regional surface nitrogen balances in intensive agricultural production systems for the period 1970-2030, Pedosphere 15 (2) (2005) 137–155.
[8] A.T. Akale, M.A. Moges, D.C. Dagnew, S.A. Tilahun, T.S. Steenhuis, Assessment of nitrate in wells and springs in the north central Ethiopian highlands, Water (Switzerland) 10 (4) (2018) 1–11, https://doi.org/10.3390/w10040476.
[9] J.K. Maghanga, J.L. Kituyi, P.O. Kisinyo, W.K. Ng'Etich, Impact of nitrogen fertilizer applications on surface water nitrate levels within a Kenyan tea plantation, J. Chem. 2013 (2013), https://doi.org/10.1155/2013/196516.
[10] D. Tolessa, C.C. Du Preez, G.M. Ceronio, Fate of nitrogen applied to maize on conventional and minimum tilled nitisols in Western Ethiopia, S. Afr. J. Plant Soil 24 (2) (2007) 77–83, https://doi.org/10.1080/02571862.2007.10634785.
[11] S.B. Wassie, Natural resource degradation tendencies in Ethiopia: a review, Environ. Syst. Res. 9 (1) (2020) 1–29, https://doi.org/10.1186/s40068-020-00194-1.
[12] M. Anas, et al., Fate of Nitrogen in Agriculture and Environment: Agronomic, Eco-Physiological and Molecular Approaches to Improve Nitrogen Use Efficiency, in: Biological Research, vol. 53, BioMed Central, 2020, pp. 1–20, https://doi.org/10.1186/s40659-020-00312-4, 1.
[13] D.L. Dinnes, et al., Nitrogen management strategies to reduce nitrate leaching in tile-drained midwestern soils, Agron. J. 94 (1) (2002) 153–171, https://doi.org/10.2134/agronj2002.1530.

[14] H.G. Kuma, F.F. Feyessa, T.A. Demissie, Land-use/land-cover changes and implications in Southern Ethiopia: evidence from remote sensing and informants, Heliyon 8 (3) (2022) e09071, https://doi.org/10.1016/j.heliyon.2022.e09071.
[15] K. Okamoto, S. Goto, T. Anzai, S. Ando, Nitrogen leaching and nitrogen balance under differing nitrogen fertilization for sugarcane cultivation on a subtropical island, Water (Switzerland) 13 (5) (2021) 1–13, https://doi.org/10.3390/w13050740.
[16] Y. Cao, Y. Tian, B. Yin, Z. Zhu, Improving agronomic practices to reduce nitrate leaching from the rice-wheat rotation system, Agric. Ecosyst. Environ. 195 (3) (2014) 61–67, https://doi.org/10.1016/j.agee.2014.05.020.
[17] U. Usman, S.A. Yelwa, S.U. Gulumbe, A. Danbaba, R. Nir, Modelling relationship between NDVI and climatic variables using geographically weighted regression, J. Math. Sci. Appl. 1 (2) (2013) 24–28, https://doi.org/10.12691/jmsa-1-2-2.
[18] H. Lee, J. Wang, B. Leblon, Using linear regression, random forests, and support vector machine with unmanned aerial vehicle multispectral images to predict canopy nitrogen weight in corn, Rem. Sens. 12 (13) (2020), https://doi.org/10.3390/rs12132071.
[19] F. Clement, D. Orange, M. Williams, C. Mulley, M. Epprecht, Drivers of afforestation in Northern Vietnam: assessing local variations using geographically weighted regression, Appl. Geogr. 29 (4) (2009) 561–576, https://doi.org/10.1016/j.apgeog.2009.01.003.
[20] A. Atabati, H. Adab, G. Zolfaghari, M. Nasrabadi, Modeling groundwater nitrate concentrations using spatial and non-spatial regression models in a semi-arid environment, Water Sci. Eng. 15 (3) (2022) 218–227, https://doi.org/10.1016/j.wse.2022.05.002.
[21] M. Imran, A. Stein, R. Zurita-Milla, Using geographically weighted regression kriging for crop yield mapping in West Africa, Int. J. Geogr. Inf. Sci. 29 (2) (2015) 234–257, https://doi.org/10.1080/13658816.2014.959522.
[22] B.D. Wardlow, S.L. Egbert, A comparison of MODIS 250-m EVI and NDVI data for crop mapping: a case study for southwest Kansas, Int. J. Rem. Sens. 31 (3) (2010) 805–830, https://doi.org/10.1080/01431160902897858.
[23] J. Penman, M. Gytarsky, T. Hiraishi, W. Irving, T. Krug, IPCC - Guidelines for National Greenhouse Gas Inventories, vol. 2006, 2006 [Online]. Available: http://www.ipcc-nggip.iges.or.jp/public/2006gl/index.html.
[24] N. Wang, Z. Yao, W. Liu, X. Lv, M. Ma, Spatial variabilities of runoff erosion and different underlying surfaces in the Xihe River basin, Water (Switzerland) 11 (2) (2019) 1–15, https://doi.org/10.3390/w11020352.
[25] Z.D. Lwimbo, H.C. Komakech, A.N.N. Muzuka, Impacts of emerging agricultural practices on groundwater quality in Kahe catchment, Tanzania, Water (Switzerland) 11 (11) (2019) 1–25, https://doi.org/10.3390/w11112263.
[26] X. Hou, et al., Detection and attribution of nitrogen runoff trend in China's croplands, Environ. Pollut. 234 (2018) 270–278, https://doi.org/10.1016/j.envpol.2017.11.052.
[27] Z. Li, et al., Regional simulation of nitrate leaching potential from winter wheat-summer maize rotation croplands on the North China Plain using the NLEAP-GIS model, Agric. Ecosyst. Environ. 294 (December 2019) (2020) 106861, https://doi.org/10.1016/j.agee.2020.106861.
[28] C.M. Lee, et al., Contribution of nitrate-nitrogen concentration in groundwater to stream water in an agricultural head watershed, Environ. Res. 184 (March) (2020) 109313, https://doi.org/10.1016/j.envres.2020.109313.
[29] H. Lyu, Z. Dong, S. Pande, Interlinkages between human agency, water use efficiency and sustainable food production, J. Hydrol. 582 (December 2019) (2020) 124524, https://doi.org/10.1016/j.jhydrol.2019.124524.
[30] FAO ASIS, "Food and Agricultural Organization (FAO), Agricultural Stress Index System (ASIS)", Crop/Pasture Phonology - Start/Maximum/End of Season, 2022, p. 2022. http://www.fao.org/giews/earthobservation/. data observed at May/2022.
[31] F. Ademe, K. Kibret, S. Beyene, G. Mitike, M. Getinet, Rainfall analysis for rain-fed farming in the great rift valley basins of Ethiopia, J. Water Clim. Chang. 11 (3) (2020) 812–828, https://doi.org/10.2166/wcc.2019.242.
[32] E.H. Koh, E. Lee, K.K. Lee, Application of geographically weighted regression models to predict spatial characteristics of nitrate contamination: implications for an effective groundwater management strategy, J. Environ. Manag. 268 (2020) 110646, https://doi.org/10.1016/j.jenvman.2020.110646.
[33] A. Bedard-Haughn, L.P. Comeau, A. Sangster, Gross nitrogen mineralization in pulse-crop rotations on the Northern Great Plains, Nutrient Cycl. Agroecosyst. 95 (2) (2013) 159–174, https://doi.org/10.1007/s10705-013-9555-z.
[34] B.N. Wolteji, S.T. Bedhadha, S.L. Gebre, E. Alemayehu, D.O. Gemeda, Multiple indices based agricultural drought assessment in the Rift Valley region of Ethiopia, Environ. Challenges 7 (December 2021) (2022) 100488, https://doi.org/10.1016/j.envc.2022.100488.
[35] T. Kätterer, et al., Biochar addition persistently increased soil fertility and yields in maize-soybean rotations over 10 years in sub-humid regions of Kenya, Field Crops Res. 235 (February) (2019) 18–26, https://doi.org/10.1016/j.fcr.2019.02.015.
[36] S.Y. Pan, K.H. He, K.T. Lin, C. Fan, C.T. Chang, Addressing nitrogenous gases from croplands toward low-emission agriculture, npj Clim. Atmos. Sci. 5 (1) (2022), https://doi.org/10.1038/s41612-022-00265-3.
[37] IPCC, N2O Emissions from Managed Soils, and CO2 Emissions from Lime and Urea Application, 2006.
[38] L. Wang, H. Zheng, H. Zhao, B.E. Robinson, Nitrogen balance dynamics during 2000-2010 in the Yangtze River Basin croplands, with special reference to the relative contributions of cropland area and synthetic fertilizer N application rate changes, PLoS One 12 (7) (2017) 1–17, https://doi.org/10.1371/journal.pone.0180613.
[39] L. Xue, Z. Hao, T. Huo, D. Li, The distributed stochastic monitoring and modeling on non-point source pollution and water ecosystem health assessment BT - 2nd International Conference on Bioinformatics and Biomedical Engineering, iCBBE 2008 (50609006) (2008) 4263–4266, https://doi.org/10.1109/ICBBE.2008.566. May 16, 2006 - May 18, 2006.
[40] IPCC, (IPCC-EFDB) User Manual and Database on Greenhouse Gas Emission Factors, 2020 [Online]. Available: http://www.ipcc-nggip.iges.or.jp/EFDB/main.php (Version).
[41] S. Wang, P. Rao, D. Yang, L. Tang, A combination model for quantifying non-point source pollution based on land use type in a typical urbanized area, Water (Switzerland) 12 (3) (2020) 1–18, https://doi.org/10.3390/w12030729.
[42] C. Schurz, et al., A comprehensive sensitivity and uncertainty analysis for discharge and nitrate-nitrogen loads involving multiple discrete model inputs under future changing conditions, Hydrol. Earth Syst. Sci. 23 (3) (2019) 1211–1244, https://doi.org/10.5194/hess-23-1211-2019.
[43] T.E. Lychuk, R.L. Hill, R.C. Izaurralde, B. Momen, A.M. Thomson, Evaluation of climate change impacts and effectiveness of adaptation options on nitrate loss , microbial respiration , and soil organic carbon in the Southeastern USA, Agric. Syst. 193 (2021) 103210, https://doi.org/10.1016/j.agsy.2021.103210.
[44] J.T. Waddell, R.R. Weil, Effects of fertilizer placement on solute leaching under ridge tillage and no tillage, Soil Tillage Res. 90 (1–2) (2006) 194–204, https://doi.org/10.1016/j.still.2005.09.002.
[45] L. Lassaletta, et al., Nitrogen dynamics in cropping systems under Mediterranean climate: a systemic analysis, Environ. Res. Lett. 16 (7) (2021), https://doi.org/10.1088/1748-9326/ac002c.
[46] M.G. Genjebo, A. Kemal, A.S. Nannawo, Assessment of surface water resource and allocation optimization for diverse demands in Ethiopia's upper Bilate Watershed, Heliyon 9 (10) (2023) e20298, https://doi.org/10.1016/j.heliyon.2023.e20298.
[47] CSA, Woreda -Level Crop Production Rankings in Ethiopia : A Pooled Data Approach James Warner Tim Stehulak Leulsegged Kasa International Food Policy Research Institute (IFPRI) Addis Ababa , Ethiopia, 2015.
[48] USAID, Ethiopia Southern Nations , Nationalities and Peoples Region (SNNPR) Livelihood Zone Reports, 2005 [Online]. Available: https://pdf.usaid.gov/pdf_docs/PNADJ867.pdf.
[49] M.L. Mann, J.M. Warner, Ethiopian wheat yield and yield gap estimation: a spatially explicit small area integrated data approach, Field Crops Res. 201 (2017) 60–74, https://doi.org/10.1016/j.fcr.2016.10.014.
[50] M. Roznik, M. Boyd, L. Porth, Improving crop yield estimation by applying higher resolution satellite NDVI imagery and high-resolution cropland masks, Remote Sens. Appl. Soc. Environ. 25 (October 2021) (2022) 100693, https://doi.org/10.1016/j.rsase.2022.100693.
[51] N.E.T. Fews, Ethiopia livelihood zones. *https://fews.net/fews-data/335*, 2018. (Accessed 30 July 2020).
[52] K. Didan, MOD13Q1 MODIS/Terra Vegetation Indices 16-Day L3 Global 250m SIN Grid V006 [Data Set]. NASA EOSDIS Land Processes DAAC, 2015, https://doi.org/10.5067/MODIS/MOD13Q1.006 from. (Accessed 27 May 2022).

[53] A. Mechal, T. Wagner, S. Birk, Recharge variability and sensitivity to climate: the example of gidabo river basin, main Ethiopian rift, J. Hydrol. Reg. Stud. 4 (2015) 644–660, https://doi.org/10.1016/j.ejrh.2015.09.001.
[54] F. Xie, H. Fan, Deriving drought indices from MODIS vegetation indices (NDVI/EVI) and Land Surface Temperature (LST): is data reconstruction necessary? Int. J. Appl. Earth Obs. Geoinf. 101 (2021) 102352 https://doi.org/10.1016/j.jag.2021.102352.
[55] B.G. Assa, A. Bhowmick, B.E. Cholo, Modeling nitrogen balance for pre-assessment of surface and groundwater nitrate (NO3-−N) contamination from N–fertilizer application loss: a case of the bilate downstream watershed cropland, Water. Air. Soil Pollut. 234 (2) (2023), https://doi.org/10.1007/s11270-023-06114-0.
[56] J. Liu, T. Huffman, J. Shang, B. Qian, T. Dong, Y. Zhang, Identifying major crop types in eastern Canada using a fuzzy decision tree classifier and phenological indicators derived from time series MODIS data, Can. J. Rem. Sens. 42 (3) (2016) 259–273, https://doi.org/10.1080/07038992.2016.1171133.
[57] D. Sulla-menashe, et al., MODIS collection 5 global land cover : algorithm refinements and characterization of new datasets remote sensing of environment MODIS collection 5 global land cover : algorithm re fi nements and characterization of new datasets, Remote Sens. Environ. 114 (1) (2010) 168–182, https://doi.org/10.1016/j.rse.2009.08.016.
[58] J. Gray, D. Sulla-Menashe, M.A. Friedl, User guide to collection 6 MODIS land cover dynamics (MCD12Q2) product, User Guid 6 (Figure 1) (2019) 1–8, https://doi.org/10.5067/MODIS/MCD12Q1.006 [Online]. Available:.
[59] N.H. Batjes, IPCC Default Soil Classes Derived from the Harmonized World Soil Data Base (Ver. 1.0). Report 2009/02, Carbon Benefits Project (CBP) and ISRIC - World Soil Information, Wageningan (With dataset).," *Africa (Lond).*, No. October, 2009 [Online]. Available: http://www.isric.org/isric/Webdocs/Docs/ISRIC_Report_2009_02.pdf.
[60] R. Van Hoolst, et al., FAO's AVHRR-based Agricultural Stress Index System (ASIS) for global drought monitoring, Int. J. Rem. Sens. 37 (2) (2016) 418–439, https://doi.org/10.1080/01431161.2015.1126378.
[61] H.R. Bedane, K.T. Beketie, E.E. Fantahun, G.L. Feyisa, F.A. Anose, The impact of rainfall variability and crop production on vertisols in the central highlands of Ethiopia, Environ. Syst. Res. 11 (1) (2022), https://doi.org/10.1186/s40068-022-00275-3.
[62] J. Liu, W. Zhu, C. Atzberger, A. Zhao, Y. Pan, X. Huang, A phenology-based method to map cropping patterns under a wheat-maize rotation using remotely sensed time-series data, Rem. Sens. 10 (8) (2018) 1–25, https://doi.org/10.3390/rs10081203.
[63] D. Rijks, M. Massart, F. Rembold, R. Gommes, O. Léo, The 2nd International Workshop on Crop and Rangeland Monitoring in Eastern Africa, 2007, https://doi.org/10.2788/17052.
[64] T. Dong, et al., Field-scale crop seeding date estimation from MODIS data and growing degree days in Manitoba, Canada, Rem. Sens. 11 (15) (2019), https://doi.org/10.3390/rs11151760.
[65] NMSA, National metrological services agency agrometeorological bulletin, Seas. Agro Meterological Bull. Bega,2004/05 15 (3) (2005) 1–19 [Online]. Available: http://www.wamis.org/countries/ethiopia/Eth20051503.pdf.
[66] M.L. Edamo, K.M. Bushira, T.Y. Ukumo, M.A. Ayele, M.A. Alaro, H.B. Borko, Effect of climate change on water availability in Bilate catchment, Southern Ethiopia, Water Cycle 3 (2022) 86–99, https://doi.org/10.1016/j.watcyc.2022.06.001.
[67] Y.A. Orke, M.H. Li, Hydroclimatic variability in the bilate watershed, Ethiopia, Climate 9 (6) (2021) 1–23, https://doi.org/10.3390/cli9060098.
[68] B.T. Lambe, S. Kundapura, Analysis of meteorological variability and tendency over Bilate basin of Rift Valley Lakes basins in Ethiopia, Arabian J. Geosci. 14 (23) (2021), https://doi.org/10.1007/s12517-021-08962-8.
[69] B.D. Wardlow, S.L. Egbert, J.H. Kastens, Analysis of time-series MODIS 250 m vegetation index data for crop classification in the U.S. Central Great Plains, Remote Sens. Environ. 108 (3) (2007) 290–310, https://doi.org/10.1016/j.rse.2006.11.021.
[70] A.A. Mekonen, A.B. Berlie, Rural households' livelihood vulnerability to climate variability and extremes: a livelihood zone-based approach in the Northeastern Highlands of Ethiopia, Ecol. Process. 10 (1) (2021), https://doi.org/10.1186/s13717-021-00313-5.
[71] D.A. Ali, K. Deininger, D. Monchuk, Using satellite imagery to assess impacts of soil and water conservation measures: evidence from Ethiopia's Tana-Beles watershed, Ecol. Econ. 169 (January) (2020), https://doi.org/10.1016/j.ecolecon.2019.106512.
[72] R. Remesan, I.P. Holman, Effect of baseline meteorological data selection on hydrological modelling of climate change scenarios, J. Hydrol. 528 (2015) 631–642, https://doi.org/10.1016/j.jhydrol.2015.06.026.
[73] A.S. Ribeiro, et al., Role of measurement uncertainty in the comparison of average areal rainfall methods, Metrologia 58 (4) (2021), https://doi.org/10.1088/1681-7575/ac0d49.
[74] A.H. Chotangui, et al., Evaluation of NO3-N leaching in commercial fields of leafy vegetables by the soil nitrogen balance estimation system, Environ. Control Biol. 53 (3) (2015) 145–157, https://doi.org/10.2525/ecb.53.145.
[75] W. Negash, Catchment dynamics and its impact on runoff generation: coupling watershed modelling and statistical analysis to detect catchment responses, Int. J. Water Resour. Environ. Eng. 6 (2) (2014) 73–87, https://doi.org/10.5897/ijwree2013.0449.
[76] J. Xue, Z. Huo, I. Kisekka, Assessing impacts of climate variability and changing cropping patterns on regional evapotranspiration, yield and water productivity in California's San Joaquin watershed, Agric. Water Manag. 250 (January) (2021) 106852, https://doi.org/10.1016/j.agwat.2021.106852.
[77] Z.H. Wang, S.X. Li, Nitrate N Loss by Leaching and Surface Runoff in Agricultural Land: A Global Issue (A Review), first ed., vol. 156, Elsevier Inc., 2019 https://doi.org/10.1016/bs.agron.2019.01.007.
[78] T. Condom, et al., Climatological and hydrological observations for the south American andes: in situ stations, satellite, and reanalysis data sets, Front. Earth Sci. 8 (April) (2020) 1–20, https://doi.org/10.3389/feart.2020.00092.
[79] T. Zhang, B. Li, J. Wang, M. Hu, L. Xu, Estimation of Areal mean rainfall in remote areas using b-shade model, Adv. Meteorol. 2016 (2016) 8–11, https://doi.org/10.1155/2016/7643753.
[80] R. Arsenault, F. Brissette, Determining the optimal spatial distribution of weather station networks for hydrological modeling purposes using rcm datasets: an experimental approach, J. Hydrometeorol. 15 (1) (2014) 517–526, https://doi.org/10.1175/JHM-D-13-088.1.
[81] A. Molla, L. Di, L. Guo, C. Zhang, F. Chen, Spatio-temporal responses of precipitation to urbanization with google earth engine: a case study for lagos, Nigeria, Urban Sci 6 (2) (2022) 40, https://doi.org/10.3390/urbansci6020040.
[82] A. Banerjee, R. Chen, M.E. Meadows, R.B. Singh, S. Mal, D. Sengupta, An analysis of long-term rainfall trends and variability in the uttarakhand himalaya using google earth engine, Rem. Sens. 12 (4) (2020), https://doi.org/10.3390/rs12040709.
[83] D. Ahsan, U.S. Brandt, H. Faruque, Local agricultural practices to adapt with climate change. Is sustainability a priority? Curr. Res. Environ. Sustain. 3 (2021) 100065 https://doi.org/10.1016/j.crsust.2021.100065.
[84] C. Funk, et al., The climate hazards infrared precipitation with stations - a new environmental record for monitoring extremes, Sci. Data 2 (2015) 1–21, https://doi.org/10.1038/sdata.2015.66.
[85] M. Cheng, et al., Performance assessment of spatial interpolation of precipitation for hydrological process simulation in the Three Gorges Basin, Water (Switzerland) 9 (11) (2017), https://doi.org/10.3390/w9110838.
[86] D. Dimov, et al., Framework for agricultural performance assessment based on MODIS multitemporal data, J. Appl. Remote Sens. 13 (2) (2019) 1, https://doi.org/10.1117/1.jrs.13.025501.
[87] P. Mab, S. Ly, C. Chompuchan, E. Kositsakulchai, Evaluation of satellite precipitation from google earth engine in tonle sap basin, Cambodia, THA 2019 Int. Conf. Water Manag. Clim. Chang. Towar. Asia's Water-Energy-Food Nexus SDGs 2019 (July) (2019). January 23-25.
[88] R. Valencia Cotera, L. Guillaumot, R.K. Sahu, C. Nam, L. Lierhammer, M. Máñez Costa, An assessment of water management measures for climate change adaptation of agriculture in Seewinkel, Sci. Total Environ. 885 (September 2022) (2023), https://doi.org/10.1016/j.scitotenv.2023.163906.
[89] M. Edmond Moeletsi, Z. Phumlani Shabalala, G. De Nysschen, S. Walker, Evaluation of an inverse distance weighting method for patching daily and dekadal rainfall over the free state province, South Africa, WaterSA 42 (3) (2016) 466–474, https://doi.org/10.4314/wsa.v42i3.12.
[90] G. Bayable, G. Amare, G. Alemu, T. Gashaw, Spatiotemporal variability and trends of rainfall and its association with pacific ocean sea surface temperature in west harerge zone, eastern Ethiopia, Environ. Syst. Res. 10 (1) (2021), https://doi.org/10.1186/s40068-020-00216-y.

[91] J. Wang, et al., Ensemble machine-learning-based framework for estimating total nitrogen concentration in water using drone-borne hyperspectral imagery of emergent plants: a case study in an arid oasis, NW China, Environ. Pollut. 266 (2020) 115412, https://doi.org/10.1016/j.envpol.2020.115412.

[92] C.Y. Liu, P. Aryastana, G.R. Liu, W.R. Huang, Assessment of satellite precipitation product estimates over Bali Island, Atmos. Res. 244 (May) (2020) 105032, https://doi.org/10.1016/j.atmosres.2020.105032.

[93] B.S. Wiwoho, I.S. Astuti, I.A.G. Alfarizi, H.R. Sucahyo, Validation of three daily satellite rainfall products in a humid tropic watershed, brantas, Indonesia: implications to land characteristics and hydrological modelling, Hydrology 8 (4) (2021), https://doi.org/10.3390/hydrology8040154.

[94] H. Bayraktar, F.S. Turalioglu, Z. Şen, The estimation of average areal rainfall by percentage weighting polygon method in Southeastern Anatolia Region, Turkey, Atmos. Res. 73 (1–2) (2005) 149–160, https://doi.org/10.1016/j.atmosres.2004.08.003.

[95] Y. Yao, Q. Dai, R. Gao, Y. Gan, X. Yi, Effects of rainfall intensity on runoff and nutrient loss of gently sloping farmland in a karst area of SW China, PLoS One 16 (3 March) (2021) 1–18, https://doi.org/10.1371/journal.pone.0246505.

[96] L. Feng, Y. Wang, Z. Zhang, Q. Du, Geographically and temporally weighted neural network for winter wheat yield prediction, Remote Sens. Environ. 262 (April) (2021) 112514, https://doi.org/10.1016/j.rse.2021.112514.

[97] D. Friedl, M. Sulla-Menashe, MCD12Q1 MODIS/Terra+Aqua Land Cover Type Yearly L3 Global 500m SIN Grid V006 [Data Set]. NASA EOSDIS Land Processes DAAC, NASA EOSDIS L. Process. DAAC, 2019, pp. 2003–2005, https://doi.org/10.5067/MODIS/MCD12Q1.006. (Accessed 2 February 2022). no. 8.5.2017.

[98] F.H. Evans, A.R. Salas, S. Rakshit, C.A. Scanlan, S.E. Cook, Assessment of the use of geographically weighted regression for analysis of large on-farm experiments and implications for practical application, Agronomy 10 (11) (2020), https://doi.org/10.3390/agronomy10111720.

[99] J. Song, H. Yu, Y. Lu, Spatial-scale dependent risk factors of heat-related mortality: a multiscale geographically weighted regression analysis, Sustain. Cities Soc. 74 (July) (2021), https://doi.org/10.1016/j.scs.2021.103159.

[100] U. Usman, S.A. Yelwa, U. Gulumbe, A. Danbaba, "Modelling Relationship between NDVI and Climatic Variables Using Geographically Weighted Regression," (March 2017) (2013), https://doi.org/10.12691/jmsa-1-2-2.

[101] A. Katebikord, S.H. Sadeghi, V.P. Singh, Spatial modeling of soil organic carbon using remotely sensed indices and environmental field inventory variables, Environ. Monit. Assess. 194 (3) (2022), https://doi.org/10.1007/s10661-022-09842-8.

[102] L. Yuan, T. Sinshaw, K.J. Forshay, Review of watershed-scale water quality and nonpoint source pollution models, Geosci. 10 (1) (2020) 1–33, https://doi.org/10.3390/geosciences10010025.

[103] J.B. Nippert, et al., Linking plant growth responses across topographic gradients in tallgrass prairie, Oecologia 166 (4) (2011) 1131–1142, https://doi.org/10.1007/s00442-011-1948-6.

[104] Y. Chen, M. Li, K. Su, X. Li, Spatial-temporal characteristics of the driving factors of agricultural carbon emissions: empirical evidence from Fujian, China, Energies 12 (16) (2019), https://doi.org/10.3390/en12163102.

[105] Z. Zhao, J. Gao, Y. Wang, J. Liu, S. Li, Exploring spatially variable relationships between NDVI and climatic factors in a transition zone using geographically weighted regression, Theor. Appl. Climatol. 120 (3–4) (2015) 507–519, https://doi.org/10.1007/s00704-014-1188-x.

[106] B. Lu, M. Charlton, P. Harris, A.S. Fotheringham, Geographically weighted regression with a non-Euclidean distance metric: a case study using hedonic house price data, Int. J. Geogr. Inf. Sci. 28 (4) (2014) 660–681, https://doi.org/10.1080/13658816.2013.865739.

[107] L.P. Lugoi, Y. Bamutaze, V. Martinsen, B. Dick, R. Almås, Ecosystem productivity response to environmental forcing, prospect for improved rain-fed cropping productivity in lake Kyoga Basin, Appl. Geogr. 102 (November 2018) (2019) 1–11, https://doi.org/10.1016/j.apgeog.2018.11.001.

[108] J.H. Grove, E.M. Pena-Yewtukhiw, Guiding cover crop establishment to scavenge residual soil nitrate nitrogen using site-specific approaches, Adv. Anim. Biosci. 8 (2) (2017) 293–298, https://doi.org/10.1017/s2040470017000796.

[109] A.T. Austin, et al., Water pulses and biogeochemical cycles in arid and semiarid ecosystems, Oecologia 141 (2) (2004) 221–235, https://doi.org/10.1007/s00442-004-1519-1.

[110] Food security information network(FSIN), Global Report on Food Crises, 2021 [Online]. Available: https://www.wfp.org/publications/2020-global-report-food-crises.

[111] Q. Zhou, A. Ismaeel, Geo-spatial Information Science Integration of maximum crop response with machine learning regression model to timely estimate crop yield, Geo-Spatial Inf. Sci. 00 (00) (2021) 1–10, https://doi.org/10.1080/10095020.2021.1957723.

[112] F. Zhang, G. Zhou, Estimation of vegetation water content using hyperspectral vegetation indices: a comparison of crop water indicators in response to water stress treatments for summer maize, BMC Ecol. 19 (1) (2019) 1–12, https://doi.org/10.1186/s12898-019-0233-0.

[113] T. Mulualem, et al., Exploring the variability of soil nutrient outflows as influenced by land use and management practices in contrasting agro-ecological environments, Sci. Total Environ. 786 (April) (2021) 147450, https://doi.org/10.1016/j.scitotenv.2021.147450.

[114] G. Zhang, et al., Mapping paddy rice planting areas through time series analysis of MODIS land surface temperature and vegetation index data, ISPRS J. Photogrammetry Remote Sens. 106 (2015) 157–171, https://doi.org/10.1016/j.isprsjprs.2015.05.011.

[115] N. Pasqualotto, J. Delegido, S. Van Wittenberghe, J. Verrelst, J.P. Rivera, J. Moreno, Retrieval of canopy water content of different crop types with two new hyperspectral indices: water Absorption Area Index and Depth Water Index, Int. J. Appl. Earth Obs. Geoinf. 67 (October 2017) (2018) 69–78, https://doi.org/10.1016/j.jag.2018.01.002.

[116] F. Li, et al., Remotely estimating aerial N status of phenologically differing winter wheat cultivars grown in contrasting climatic and geographic zones in China and Germany, Field Crops Res. 138 (2012) 21–32, https://doi.org/10.1016/j.fcr.2012.09.002.

[117] Z. Chen, S. Zhang, W. Geng, Y. Ding, X. Jiang, Use of Geographically Weighted Regression (GWR) to Reveal Spatially Varying Relationships between Cd Accumulation and Soil Properties at Field Scale, no. Cd, 2022.

[118] K.S. Kibret, C. Marohn, G. Cadisch, Use of MODIS EVI to map crop phenology, identify cropping systems, detect land use change and drought risk in Ethiopia–an application of Google Earth Engine, Eur. J. Remote Sens. 53 (1) (2020) 176–191, https://doi.org/10.1080/22797254.2020.1786466.

[119] K. Didan, A.B. Munoz, R. Solano, A. Huete, MODIS Vegetation Index User 's Guide, Collection 6), 2015.

[120] H. Gao, Q. Tang, X. Shi, C. Zhu, T. Bohn, F. Su, Water budget record from variable infiltration capacity (VIC) model algorithm theoretical basis document, in: *Rapport - Version 1.2*, No, Vic, University of Washington Seattle, WA, 2009, p. 57, 98195.

[121] M.M. Nistor, A. Satyanaga, Ş. Dezsi, I. Haidu, European Grid dataset of actual evapotranspiration, water availability and effective precipitation, Atmosphere 13 (5) (2022), https://doi.org/10.3390/atmos13050772.

[122] S. Tamagno, et al., Predicting nitrate leaching loss in temperate rainfed cereal crops: relative importance of management and environmental drivers, Environ. Res. Lett. 17 (6) (2022) 064043, https://doi.org/10.1088/1748-9326/ac70ee.

[123] A. Nowakowski, et al., Crop type mapping by using transfer learning, Int. J. Appl. Earth Obs. Geoinf. 98 (February) (2021) 102313, https://doi.org/10.1016/j.jag.2021.102313.

[124] E. Babaeian, M. Sadeghi, S.B. Jones, C. Montzka, H. Vereecken, M. Tuller, Ground, proximal, and satellite remote sensing of soil moisture, Rev. Geophys. 57 (2) (2019) 530–616, https://doi.org/10.1029/2018RG000618.

[125] K. Didan, A.B. Munoz, R. Solano, A. Huete, MODIS Vegetation Index User's Guide (MOD13 Series) Version 3.0 Ccollection 6, vol. 2015, 2015, p. 38. May.

[126] E.R. Hunt Jr., J.J. Qu, X. Hao, L. Wang, Remote sensing of canopy water content: scaling from leaf data to MODIS, Remote Sens. Model. Ecosyst. Sustain. VI 7454 (August) (2009) 745409, https://doi.org/10.1117/12.825401.

[127] R. Kozłowski, R. Kruszyk, S. Małek, The effect of environmental conditions on pollution deposition and canopy leaching in two pine stands (West Pomerania and Świetokrzyskie mountains, Poland), Forests 11 (5) (2020), https://doi.org/10.3390/F11050535.

[128] T. Tadesse, G.B. Senay, G. Berhan, T. Regassa, S. Beyene, Evaluating a satellite-based seasonal evapotranspiration product and identifying its relationship with other satellite-derived products and crop yield: a case study for Ethiopia, Int. J. Appl. Earth Obs. Geoinf. 40 (2015) 39–54, https://doi.org/10.1016/j.jag.2015.03.006.

[129] R. Duffková, J. Holub, P. Fucík, J. Rožnovský, I. Novotnỳ, Long-term water balance of selected field crops in different agricultural regions of the Czech republic using fao-56 and soil hydrological approaches, Sustain. Times 11 (19) (2019), https://doi.org/10.3390/su11195243.

[130] J. Telo da Gama, L. Loures, A. Lopez-Piñeiro, D. Quintino, P. Ferreira, J.R. Nunes, Assessing the long-term impact of traditional agriculture and the mid-term impact of intensification in face of local climatic changes, Agric. For. 11 (9) (2021), https://doi.org/10.3390/AGRICULTURE11090814.
[131] K.A. Mir, G. Change, I. Studies, P. Purohit, IPCC 2006 Guidelines Can Change National Greenhouse Gas Inventories, 2021.
[132] P. Heffer, H. Magen, R. Mikkelsen, D. Wichelns, Managing Water and Fertilizer for Sustainable Agricultural Intensification, 2015.
[133] P. Khanthavong, S. Yabuta, H. Asai, M.A. Hossain, I. Akagi, J.I. Sakagami, Root response to soil water status via interaction of crop genotype and environment, Agronomy 11 (4) (2021) 1–15, https://doi.org/10.3390/agronomy11040708.
[134] J. Mas-Pla, A. Menció, Groundwater nitrate pollution and climate change: learnings from a water balance-based analysis of several aquifers in a western Mediterranean region (Catalonia), Environ. Sci. Pollut. Res. 26 (3) (2019) 2184–2202, https://doi.org/10.1007/s11356-018-1859-8.
[135] A. Pradipta, et al., Precision agriculture — Part 2 : irrigation management, Water (2022) 1–25.
[136] S. Dubey, H. Gupta, M.K. Goyal, N. Joshi, Evaluation of precipitation datasets available on Google earth engine over India, Int. J. Climatol. 41 (10) (2021) 4844–4863, https://doi.org/10.1002/joc.7102.
[137] G. Bariamis, E. Baltas, Hydrological modeling in agricultural intensive watershed: the case of upper east fork white river, USA, Hydrology 8 (3) (2021), https://doi.org/10.3390/hydrology8030137.
[138] S.B. Kimbi, et al., Nitrate Contamination in Groundwater : Evaluating the Effects of Demographic Aging and Depopulation in an Island with Intensive Citrus Cultivation, 2022, https://doi.org/10.3390/w14142277.
[139] R.L. Whetton, M.A. Harty, N.M. Holden, Communicating nitrogen loss mechanisms for improving nitrogen use efficiency management, focused on global wheat, Nitrogen 3 (2) (2022) 213–246, https://doi.org/10.3390/nitrogen3020016.
[140] V. Novák, H. Hlaváčiková, Soil-water content and its measurement, in: Theory and Applications of Transport in Porous Media, vol. 32, 2019, pp. 49–61, https://doi.org/10.1007/978-3-030-01806-1_5.
[141] F.H. Abdel-Kader, Assessment and monitoring of land degradation in the northwest coast region, Egypt using Earth observations data, Egypt. J. Remote Sens. Sp. Sci. 22 (2) (2019) 165–173, https://doi.org/10.1016/j.ejrs.2018.02.001.
[142] V. Nangia, C. de Fraiture, H. Turral, Water quality implications of raising crop water productivity, Agric. Water Manag. 95 (7) (2008) 825–835, https://doi.org/10.1016/j.agwat.2008.02.014.
[143] H.P. Liniger, D. Cahill, W. Critchley, D. Thomas, G.W.J. van Lynden, G. Schwilch, Categorization of SWC technologies and approaches — a global need, 12th Int. Soil Conserv. Organ. Conf. III (2002) 6–12, 2002, [Online]. Available: http://www.tucson.ars.ag.gov/isco/isco12/VolumeIII/CategorizationofSWCTechnologies.pdf.
[144] E. Parizi, S.M. Hosseini, B. Ataie-Ashtiani, C.T. Simmons, Normalized difference vegetation index as the dominant predicting factor of groundwater recharge in phreatic aquifers: case studies across Iran, Sci. Rep. 10 (1) (2020) 1–19, https://doi.org/10.1038/s41598-020-74561-4.
[145] Z. Zhou, S. V Ollinger, L. Lepine, Landscape variation in canopy nitrogen and carbon assimilation in a temperate mixed forest, Oecologia 188 (2) (2018) 595–606, https://doi.org/10.1007/s00442-018-4223-2.
[146] K. Mahmud, D. Panday, A. Mergoum, A. Missaoui, Nitrogen losses and potential mitigation strategies for a sustainable agroecosystem, Sustain. Times 13 (4) (2021) 1–23, https://doi.org/10.3390/su13042400.
[147] K. Tonhauzer, P. Tonhauzer, J. Szemesová, B. Šiška, Estimation of N2O emissions from agricultural soils and determination of nitrogen leakage, Atmosphere 11 (6) (2020) 1–14, https://doi.org/10.3390/ATMOS11060552.
[148] S. qin He, R. Ma, N. na Wang, S. Wang, T. xuan Li, Z. cheng Zheng, Comparison of nitrogen losses by runoff from two different cultivating patterns in sloping farmland with yellow soil during maize growth in Southwest China, J. Integr. Agric. 21 (1) (2022) 222–234, https://doi.org/10.1016/S2095-3119(20)63496-7.
[149] S. Tamagno, et al., Predicting nitrate leaching loss in temperate rainfed cereal crops: relative importance of management and environmental drivers, Environ. Res. Lett. 17 (6) (2022), https://doi.org/10.1088/1748-9326/ac70ee.
[150] A.M. Epelde, I. Cerro, J.M. Sánchez-Pérez, S. Sauvage, R. Srinivasan, I. Antigüedad, Application du modèle SWAT à l'évaluation de l'impact des modificationss des pratiques agricoles sur la qualité de l'eau, Hydrol. Sci. J. 60 (5) (2015) 825–843, https://doi.org/10.1080/02626667.2014.967692.
[151] L. Vilmin, N. Flipo, N. Escoffier, A. Groleau, Estimation of the water quality of a large urbanized river as defined by the European WFD: what is the optimal sampling frequency? Environ. Sci. Pollut. Res. 25 (24) (2018) 23485–23501, https://doi.org/10.1007/s11356-016-7109-z.
[152] A. Rafik, et al., Groundwater level forecasting in a data-scarce region through remote sensing data downscaling, hydrological modeling, and machine learning: a case study from Morocco, J. Hydrol. Reg. Stud. 50 (November) (2023) 101569, https://doi.org/10.1016/j.ejrh.2023.101569.
[153] F.J. Yue, et al., Land use interacts with changes in catchment hydrology to generate chronic nitrate pollution in karst waters and strong seasonality in excess nitrate export, Sci. Total Environ. 696 (2019) 134062, https://doi.org/10.1016/j.scitotenv.2019.134062.
[154] C. Xiao, et al., Effects of various soil water potential thresholds for drip irrigation on soil salinity, seed cotton yield and water productivity of cotton in northwest China, Agric. Water Manag. 279 (January) (2023), https://doi.org/10.1016/j.agwat.2023.108172.
[155] H. Li, et al., An alternative water-fertilizer-saving management practice for wheat-maize cropping system in the North China Plain: based on a 4-year field study, Agric. Water Manag. 276 (September 2022) (2023) 108053, https://doi.org/10.1016/j.agwat.2022.108053.
[156] J.G.B. Leenaars, et al., Mapping rootable depth and root zone plant-available water holding capacity of the soil of sub-Saharan Africa, Geoderma 324 (March) (2018) 18–36, https://doi.org/10.1016/j.geoderma.2018.02.046.
[157] N. Zhao, Y. Yang, X. Zhou, Application of geographically weighted regression in estimating the effect of climate and site conditions on vegetation distribution in Haihe Catchment, China, Plant Ecol. 209 (2) (2010) 349–359, https://doi.org/10.1007/s11258-010-9769-y.
[158] S.H. Yang, et al., Mapping topsoil electrical conductivity by a mixed geographically weighted regression kriging: a case study in the Heihe River Basin, northwest China, Ecol. Indicat. 102 (February) (2019) 252–264, https://doi.org/10.1016/j.ecolind.2019.02.038.
[159] M. Meroni, M.M. Verstraete, F. Rembold, F. Urbano, F. Kayitakire, A phenology-based method to derive biomass production anomalies for food security monitoring in the Horn of Africa, Int. J. Rem. Sens. 35 (7) (2014) 2472–2492, https://doi.org/10.1080/01431161.2014.883090.
[160] Z. Sun, et al., Evapotranspiration estimation based on the SEBAL model in the nansi lake wetland of China, Math. Comput. Model. 54 (3–4) (2011) 1086–1092, https://doi.org/10.1016/j.mcm.2010.11.039.